

# Tungsten Wire—From Lamp Filaments to Reinforcement Fibers for Composites in Fusion Reactors

Johann Riesch,<sup>\*</sup> Maximilian Fuhr,<sup>\*</sup> and Jürgen Almanstötter<sup>\*</sup>

The use of drawn tungsten wire marked a breakthrough in electric lighting which led to a significant advancement in human society and technology. Nowadays, thermal light sources using tungsten filaments are being more and more replaced by semiconductor-based light-emitting diodes (LEDs). Despite the lower visibility of incandescent lamps in everyday life, new markets and applications for drawn tungsten wires are opening up, which makes this complex material a highly-studied subject. One of these applications is the use of heavily drawn tungsten wires as high-performance reinforcement fibers for new composites that can withstand the extreme environment present in a nuclear fusion reactor. The main advantage of tungsten wires for this class of composites is their ductility and high strength. The wires can be used to increase the high-temperature strength of copper-based heat sink materials as well as the fracture toughness of bulk tungsten considered for the use of highly loaded reactor wall components. These new applications for tungsten wire have also given new impetus to the study of their fundamental properties.

converting electrical energy into visible light than incandescent lamps, thermal light sources using tungsten filaments dominated the general lighting market (see e.g. ref. [1] for a historical overview). The phase-out of incandescent lamps is accelerated by political decisions in several countries aiming at energy saving in order to battle man-made climate change.<sup>[2]</sup> However, tungsten filaments are still used in thermal light sources for automotive applications, for example, high-performance halogen bulbs in main beam and/or low beam, stop lamps or indicator lamps. When used as filaments in incandescent and halogen lamps, tungsten wires have to withstand temperatures above 2500 °C<sup>[3]</sup> for long times without excessive plastic deformation by creep. Thus, the main focus of tungsten wire development has been to generate a creep-resistant microstructure.

Along the processing route consisting of sintering a pure or doped tungsten powder and working the resulting material by different thermo-mechanical steps into a thin wire, the microstructure and in turn the mechanical properties of tungsten wire change drastically: Being brittle and comparably weak at low homologous temperatures before drawing, heavily drawn wires offer a very high tensile strength and can be deformed ductile even at cryogenic temperatures.<sup>[4,5]</sup> In addition, the microstructure of doped materials exhibits a very high thermal stability.

This unique set of properties makes drawn tungsten wires an attractive material for reinforcing weak or brittle matrices in fiber-reinforced composites. The first research into this field was conducted by NASA back in the 1960s (see ref. [6] and references therein). From a materials scientific point of view, the development of materials for space flight applications in the framework of the 20<sup>th</sup> century's space race is closely related to the search for suitable materials that can withstand the harsh environment present in a nuclear fusion reactor. In this context, tungsten fiber-reinforced composites are now being considered for the most highly loaded components of such reactors.<sup>[7]</sup> The role of drawn tungsten wires in these composites for fusion applications is two-fold: For heat sink applications, the wires are required to increase the high-temperature strength of the utilized copper materials. For the armor components that are in direct contact with the plasma present in a fusion reactors, the wires are used to toughen an otherwise brittle tungsten matrix. In order to optimize these new composite classes and to understand their properties, basic research efforts have been directed to improving the understanding of the unique properties

## 1. Introduction


Electric lighting is an advancement in human history that has significantly altered society's reliance on fire, torches, candles, oil lamps, and gas lamps for artificial illumination. Unarguably, no other single invention has spurred the industrial revolution and elevated the standard of living to the extent that electric lighting has. Until the development of semiconductor-based light-emitting diodes (LEDs) which are more efficient at

---

J. Riesch, M. Fuhr  
Max Planck Institute for Plasma Physics  
Boltzmannstr. 2, 85748 Garching, Germany  
E-mail: johann.riesch@ipp.mpg.de; Maximilian.Fuhr@ipp.mpg.de

M. Fuhr  
Technical University of Munich  
Boltzmannstr. 15, 85748 Garching, Germany

J. Almanstötter  
AMS OSRAM, AMSP LF PRE DMET  
Mittelstetter Weg 2, 86830 Schwabmünchen, Germany  
E-mail: Juergen.Almanstoetter@ams-osram.com

 The ORCID identification number(s) for the author(s) of this article can be found under <https://doi.org/10.1002/adem.202400951>.

© 2024 The Author(s). Advanced Engineering Materials published by Wiley-VCH GmbH. This is an open access article under the terms of the Creative Commons Attribution License, which permits use, distribution and reproduction in any medium, provided the original work is properly cited.

DOI: 10.1002/adem.202400951

of tungsten wires and the significant change of its microstructure and deformation mechanisms during wire drawing.

In the following, we will retrace the development of drawn tungsten wires from the application as filament material in incandescent lighting to its use as reinforcement material for advanced composites for nuclear fusion applications. We will highlight the materials scientific reasons for the wires' unique properties and present a new empirical model that is able to explain the ductile nature of heavily drawn wires. Furthermore, the efforts directed towards adapting tungsten wires for their use as reinforcement fiber in different composites, e.g. the use of textile techniques, will be discussed. Finally, we will give an outlook into the potential "second life" of tungsten wires in nuclear fusion compared to their "first life" in incandescent lighting.

## 2. Evolution and Manufacturing of Tungsten Wires for Lamp Filaments

The metallurgical aspects of tungsten were pivotal in the advancement of lamp filament technology.<sup>[8]</sup> The historical progression of lamp wire has been characterized by innovative experimentation, trial-and-error processing, and inventive discoveries.<sup>[9]</sup> W. D. Coolidge<sup>[10]</sup> achieved the key invention at the beginning of the 20<sup>th</sup> century through his efforts to obtain the purest possible tungsten. The as-received impure tungsten oxide  $WO_3$  was dissolved in ammonia. From this solution, a highly purified ammonium-paratungstate (APT) powder was crystallized, which was then decomposed by heating to produce pure  $WO_3$  powder.<sup>[11]</sup> Only the powders heated in covered Battersea crucibles (clay originating from Battersea, England) resulted in filament wires that were resistant to sagging of coils in burning lamps by gravitational forces.<sup>[12]</sup> However, Coolidge was unable to identify the exact substance that had been absorbed into the tungsten oxide as "doping". Crude analysis of the clay crucible showed a high concentration of silica and alumina accompanied by other less frequent constituents. Based on these results, experiments by A. Pacz<sup>[13]</sup> led to an invention that introduced aluminum potassium silicate as a dopant through a mixing process into blue tungsten oxide powder, representing a major advancement in the properties of the final tungsten wire.

The operation temperature of tungsten filaments is in the range of about 2500–3000 °C, which is well above its recrystallization temperature.<sup>[14,15]</sup> Undoped, recrystallized wire exhibits large equiaxed grains spanning the entire wire cross-section with transverse grain boundaries perpendicular to the wire axis, presenting a bamboo-like appearance. These boundaries represent weak links (see **Figure 1**, bottom) at which the corresponding coiled filament can deform easily by grain boundary sliding under the influence of gravity. This results in excessive filament sag, distortion, and reduced lifespan. In contrast to this, doped wires exhibit an overlapping, interlocking recrystallized grain structure (see **Figure 1**, top). **Figure 2** illustrates the different microstructural evolution of undoped and doped wire leading to this final state.

The discovery of doped tungsten wire facilitated the realization of efficient gas-filled lamps with a much longer lifetime in comparison to filaments produced from other materials as well as from undoped tungsten wires.<sup>[16]</sup> However, it took several

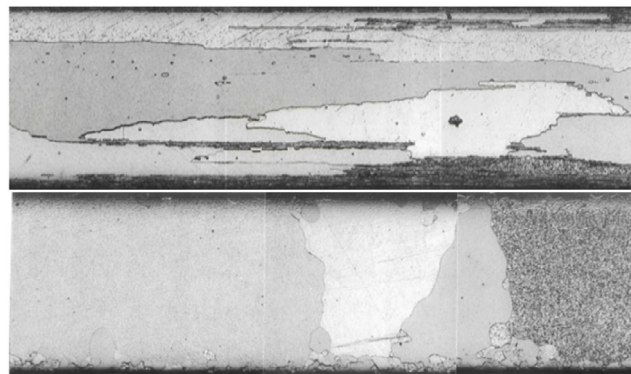


**Figure 1.** Longitudinal cross-sections of doped (top) and undoped (bottom) drawn tungsten wires (diameter 0.5 mm, OSRAM Schwabmünchen, Germany) illustrating the recrystallized microstructure after annealing at 2000 °C in pure hydrogen for 60 min. This demonstrates the effect of potassium doping on the microstructural changes upon annealing showing wavy grain boundaries and interlocking grains.

decades of material science research until the substance created by the dopant and its effects were clarified in the early 1970s.<sup>[17–21]</sup> Elemental potassium was detected within bubbles formed in doped tungsten wire by transmission electron microscopy and selected area diffraction.<sup>[22]</sup> The bubbles with radii in the range of a few nm form since the atomic radius of potassium is too large to occupy interstitial positions in the b.c.c. crystal lattice of tungsten.<sup>[23]</sup> Potassium is retained during the production process involving high temperatures although its melting point is 64 °C and its boiling point is 760 °C.<sup>[24]</sup> Nowadays, the customary starting material for the manufacturing of tungsten wire is APT crystalline powder of high purity produced from either wolframite ore ( $FeMnWO_4$ , or scheelite ore  $CaWO_4$ , by chemical extraction methods.<sup>[25]</sup> Generally, the reduction to metal powder is carried out in two stages; the first converts the APT crystals into tungsten blue oxide of nominal composition  $WO_{2.9}$  at temperatures of several hundred degrees Celsius in a mixture of nitrogen and hydrogen.<sup>[26,27]</sup> In the case of doped wire, this intermediate component incorporates the aluminum-potassium-silicate dopant.<sup>[28]</sup> The second stage converts the blue oxide to elemental metal powder by annealing at high temperatures in a hydrogen atmosphere. Depending on the type of powder that is required, it is essential to control variables such as temperature, exposure time and hydrogen flow rate. The objective is to produce a metal powder with a mean particle size of about 2–5  $\mu m$ . The actually required particle size depends on the subsequent processing, the desired bar size, and the presence or absence of dopants. For further processing into a rod, the metal powder is pressed into bars by applying high mechanical stresses.<sup>[29]</sup> To facilitate handling, the compacted and still relatively fragile bars are heated to more than 1000 °C in a hydrogen atmosphere in order to improve the bar's mechanical stability for later handling.<sup>[30]</sup> The subsequent sintering of the bars by direct resistance heating uses a similar atmosphere and temperatures above 2500 °C. Final densities up to 17.6 g cm<sup>-3</sup> and closed porosity are achieved.<sup>[31,32]</sup> In this condition, the potassium is already trapped in closed pores with a diameter of about 500 nm,<sup>[33]</sup> whereas the majority of the aluminium and silicon

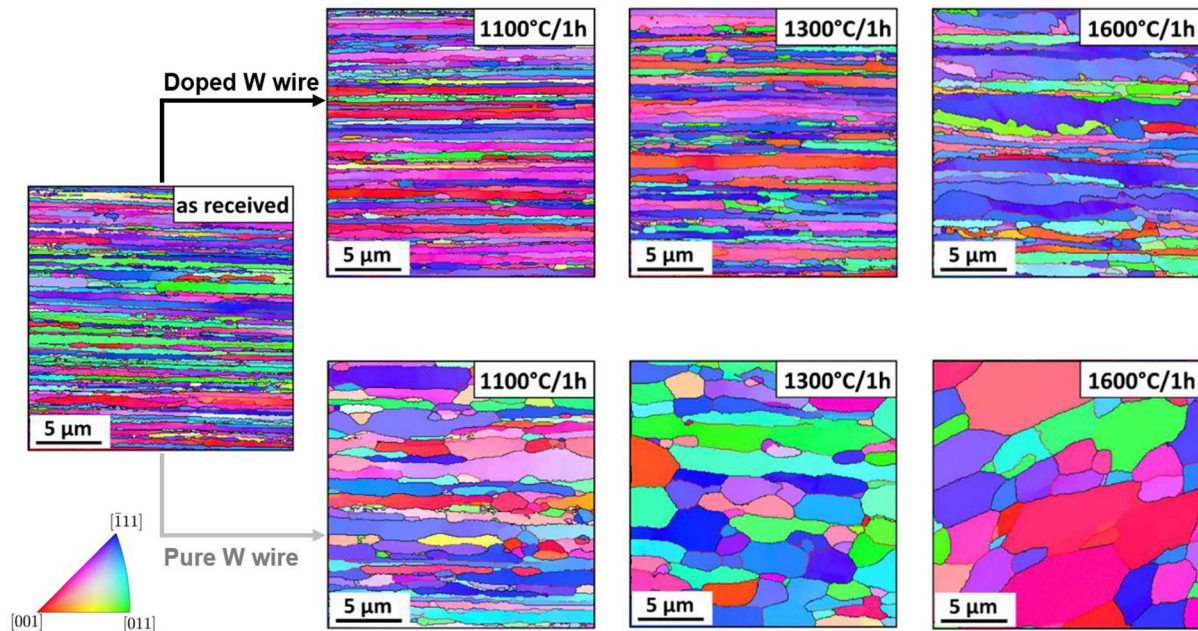


**Figure 2.** Comparison of orientation maps acquired from longitudinal cross-sections of doped (top row) and undoped (bottom row) drawn tungsten wire after isochronal annealing treatments (annealing time one hour) at temperatures up to 1600 °C (adapted from ref. [172]) using EBSD. The crystallographic orientations are coloured according to the sample z-direction (see colour key in the lower left corner). All wires were produced by OSRAM GmbH Schwabmünchen, Germany, and possess a diameter of 150 μm. (Adapted with permission.<sup>[172]</sup> Copyright 2018, Elsevier.)

is removed by volatilization, at an intermediate process state when the bar is still porous and the interconnected capillaries are open to the surface.<sup>[34]</sup> The final potassium content is usually about 75 ppm and already represents the final doping concentration found in the product (e.g., Osram, BSD-OG wire). The material is then further compacted to full density by rolling<sup>[35]</sup> and swaging.<sup>[36]</sup> Depending on the final wire diameter the thermo-mechanical processing involves more than seventy deformation steps including the process steps already mentioned and additional wire-drawing, where significant changes occur in the properties of tungsten. The main steps are schematically illustrated in **Figure 3**.

It should be noted that the conventional doping process alone is insufficient to achieve a microstructure that exhibits the characteristic interlocking grain structure in the recrystallized state. Elongation of the wire during drawing is necessary to elongate physically trapped pockets of potassium into longitudinal ribbon-shaped pipes. At elevated temperatures, these pipes break up into rows of potassium bubbles with diameters typically in the range of a few hundred angstroms.<sup>[37]</sup> The close proximity of bubble rows creates barriers against grain boundary migration and

sliding since migrating grain boundaries are pinned due to Zener pinning.<sup>[38]</sup> By this effect, the bubble rows direct the grain growth in the longitudinal direction during recrystallization and stabilize an interlocking grain structure with high aspect ratio.<sup>[39]</sup> This significantly enhances creep resistance and enables the high lifetime of coiled filaments during operation at very high temperatures.<sup>[40]</sup>

In modern tungsten wire manufacturing, the parameters associated with each processing step, especially temperature and strain, are meticulously balanced to facilitate the gradual buildup of a fine-textured, fibrous microstructure while gradually increasing the accumulated drawing (or cold-working) strain, as well as generating an effective potassium bubble dispersion within the wire. This ensures ductility at room temperature, crucial for further fabrication, where the wire must endure plastic strains of up to 30% during coiling operations, while at the same time the as-drawn microstructure is tailored to yield the interlocking and thus creep-resistant microstructure in the recrystallized state. High quality standards in the production of tungsten wires are one of the factors which for example facilitated a very recent

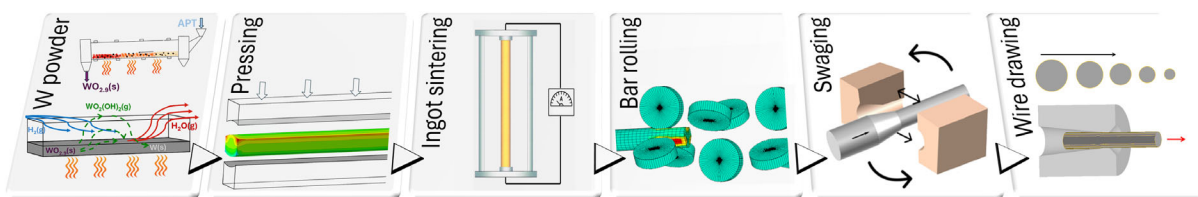


**Figure 3.** Schematic overview of the modern powder-metallurgical processing route of drawn tungsten wire. The last stage of wire drawing is applied multiple times to achieve the final diameter (represented by decreasing diameters of the circles).

realization of modern automotive halogen lamps with significantly increased performance.<sup>[41]</sup>

Besides the extremely important doping effect for lamp filaments, W. D. Coolidge<sup>[42]</sup> also laid the foundations to enable the “ductilization” of tungsten, being an inherently brittle metal at room temperature. Interestingly enough, the claims concerning ductile tungsten in the associated patent were ruled invalid in litigation. The court concluded that ductility is inherent in tungsten and that “Coolidge tungsten” is not a new metal but a discovery.<sup>[43]</sup> Thermo-mechanical working and wire drawing transforms a brittle and unworkable starting material into a strong yet ductile wire. Below temperatures of 600–700 K, tungsten exhibiting an equiaxed grain structure fractures in a brittle manner.<sup>[44,45]</sup> Above this characteristic temperature, which is referred to as ductile-to-brittle transition temperature ( $T_{DBT}$ ), tungsten can be deformed to large strains without fracture. The ductile-to-brittle transition of tungsten is influenced by a large number of extrinsic and intrinsic factors, e.g., the grain aspect ratio,<sup>[46]</sup> the grain width,<sup>[47]</sup> the dislocation density<sup>[5]</sup> as well as the strain rate during testing.<sup>[44]</sup> Wire drawing transforms the initially equiaxed grains into highly elongated fibrous ones.<sup>[48]</sup> Furthermore, a strong  $\langle 110 \rangle$  fiber texture develops.<sup>[49]</sup> It can be shown that this transformation of the microstructure and the crystallographic texture results in a shift of  $T_{DBT}$  to lower temperatures<sup>[5,50]</sup> (see **Figure 4**). Worked tungsten wire can thus be deformed plastically even at low homologous temperatures. Recrystallizing tungsten wire however leads to an increase in  $T_{DBT}$ . Excessive grain growth during secondary recrystallization (characteristic temperature:  $T_{GG}$ ) could be identified as the root cause for this phenomenon.<sup>[51]</sup> Thus, the working temperature during any thermomechanical processing of tungsten wire ( $T_D$ ) needs to be kept within the mentioned limits:  $T_{DBT} < T_D < T_{GG}$ , see **Figure 4**.

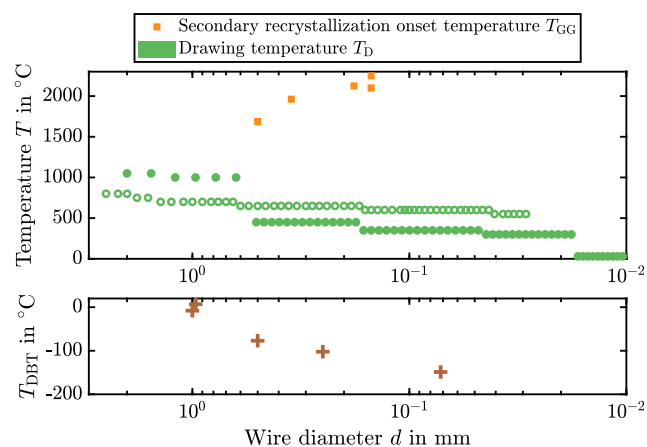


**Figure 4.** Overview on process-relevant temperatures during the manufacturing of drawn tungsten wires: The drawing temperatures (filled circles from ref. [190]; empty circles from ref. [191]) should be above the ductile-to-brittle transition temperature  $T_{DBT}$ <sup>[5,50]</sup> in order to ensure sufficient material ductility for plastic deformation and to minimize yield loss.<sup>[192]</sup> At the same time, drawing must be performed at temperatures that are low enough not to induce secondary recrystallization processes (see refs. [113,162,193,194]), which in the case of tungsten wires is linked to exaggerated grain growth and thus embrittlement.

### 3. Microstructure, Crystallographic Texture, and Mechanical Properties of Drawn Tungsten Wires

As mentioned in the previous chapter, the microstructure, crystallographic texture and mechanical properties of drawn tungsten wires are a direct result of the process details employed during their manufacturing. More specifically, the strain a wire accumulates during drawing determines its mechanical properties. Since an increase in accumulated drawing strain is intimately linked to the wire’s diameter, the diameter can be used in order to describe the microstructural, textural and property changes during drawing.

The evolution of the microstructure of drawn tungsten wires can be retraced alongside the manufacturing process: The grains of sintered tungsten are equiaxed<sup>[52]</sup> and do not possess a preferred orientation. The thermo-mechanical working by rolling and swaging leads to an elongation of the grains along the axis of the rod.<sup>[53]</sup> Simultaneously, a  $\langle 110 \rangle$  axis of the crystallites aligns with the rod axis.<sup>[53]</sup> The texture of swaged rods is described as a rather complex mixture of different superimposed cylindrical textures by Leber<sup>[54]</sup> (see also **Figure 5**). He reports different sets of cylindrical textures in swaged tungsten rods, among them a duplex of  $\langle 110 \rangle$  fibres, one of them being oriented parallel to the wire axis and one with a tilt angle of  $60^\circ$  to the wire axis. With increasing accumulated drawing strain, the cylindrical textures are transformed into a  $\langle 110 \rangle$  fiber texture. Further cold deformation by wire drawing leads to a sharpening of this characteristic texture.<sup>[53–55]</sup> Alongside this grain rotation, the grains become strongly elongated along the wire axis,<sup>[48,56,57]</sup> yielding grains with a very high aspect ratio.<sup>[55]</sup> To capture larger fraction of sample volume, neutron diffraction measurements have been conducted<sup>[58]</sup> (see **Figure 5**). The sharpening of the  $\langle 110 \rangle$  fiber texture with increasing plastic deformation was thereby confirmed. Furthermore, the grains bend around a  $\langle 110 \rangle$  axis parallel to the wire axis. When viewed along the drawing axis in a transversal cross-section, this bending of individual grains gives rise to swirly patterns designated as grain curling or alternatively Van Gogh sky structures (after V. Van Gogh’s painting “The Starry Night”). The mechanisms underlying the grain elongation and bending as well as the rise of a  $\langle 110 \rangle$  fiber texture during wire drawing have first been explained by Hosford<sup>[55]</sup> as being the consequence of grain deformation by plane strain elongation. Based on this explanation, the texture evolution has been successfully modeled by Van Houtte<sup>[59]</sup> using the relaxed constraints model.<sup>[60]</sup>

The elongated grains in drawn tungsten wires can be quantified using their width and length. Experimental evidence for the decrease in grain width during wire drawing is illustrated in **Figure 6**. Robust values for the grain length are however scarce in literature since direct measurements are challenging. This can be explained by a simple model: Assuming the grains to be perfect cylinders with an initial diameter  $D_1$  and an initial length  $L_1$ , the elongation (and thinning) during uniaxial deformation leads to a final length  $L_2$  that is given by

$$L_2 = L_1 \left( \frac{D_1}{D_2} \right)^2 \quad (1)$$

where  $D_2$  is the diameter of the cylindrical grain after deformation. Using the grain widths of a swaged tungsten rod<sup>[61]</sup> and the

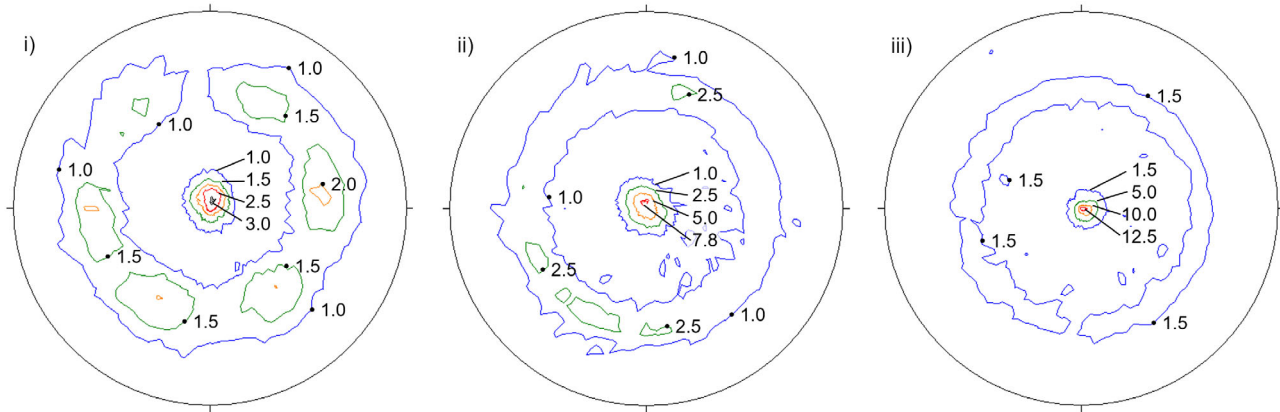


**Figure 5.** Evolution of crystallographic texture of tungsten wires during wire drawing illustrated by 110 pole figures of i) a rolled and swaged tungsten rod, ii) a tungsten wire after 28%, and iii) after 56% further reduction in wire drawing measured via neutron diffraction. Adapted with permission.<sup>[58]</sup> Copyright 2009, Elsevier.

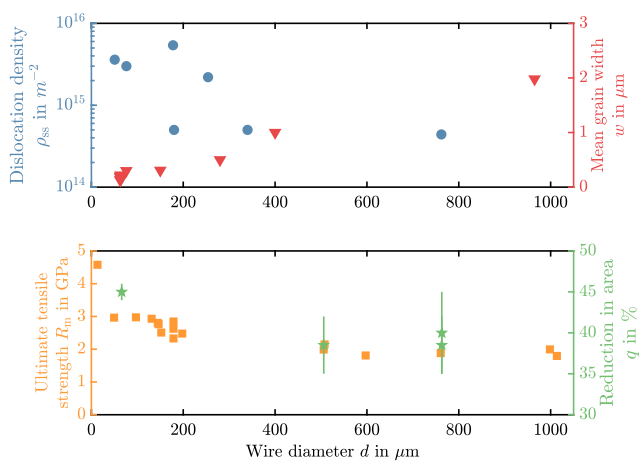


**Figure 6.** Overview on different microstructural parameters (top) and mechanical properties (bottom) of drawn tungsten wires available in literature, namely the statistically stored dislocation density  $\rho_{ss}$ <sup>[195–197]</sup> and the mean width  $w$  of elongated grains<sup>[5,57,172,198]</sup> as well as the ultimate tensile strength  $R_m$ <sup>[63,76,80,199–202]</sup> and the reduction in area  $q$ <sup>[76,78,79]</sup> observed in uniaxial tensile tests at room temperature. Note that absolute comparability among the different studies summarized here is not given since the investigated wires possess different production histories as well as chemical compositions.

thinnest wire included in Figure 6, a relative grain elongation by roughly three orders of magnitude can be expected. Such elongated grains are difficult to capture in their entirety with sufficient lateral resolution using common microscopy techniques such as scanning electron microscopy or electron backscattering diffraction (EBSD). In addition to the evolution of grain width, Figure 6 also contains data on the (statistically stored) dislocation density  $\rho_{ss}$  observed in tungsten wires with different diameters. The increase in  $\rho_{ss}$  can be rationalized by the (cold) deformation of tungsten wires during drawing.

Different plastic deformation mechanisms of drawn tungsten wires at  $T > T_{DBT}$  are discussed in literature. While some researchers assume that plastic deformation is a consequence

of dislocation activity,<sup>[62]</sup> others see indications for grain boundary sliding being the rate-controlling deformation mechanism.<sup>[63,64]</sup> A recent study by Fuhr et al.<sup>[65]</sup> could underpin the theory of dislocation-mediated plastic deformation using transient mechanical tests performed on a series of drawn doped tungsten wires. Since the tungsten wires in this study were drawn consecutively from a single sintered ingot, their chemical composition is identical and has no further influence on the deformation mechanisms relative to each other. The results of the performed strain-rate jump tests and repeated stress relaxation experiments point to the motion of screw dislocations via the kink pair mechanism,<sup>[66]</sup> i.e., the formation and propagation of kink pairs along the dislocation line, as rate-controlling deformation mechanism at  $T > T_{DBT}$ . This finding is in-line with results on the rate-controlling deformation mechanisms in rolled tungsten plates,<sup>[67,68]</sup> SPD-processed tungsten<sup>[69,70]</sup> as well as tungsten single crystals<sup>[44,71,72]</sup> and (coarse-grained) polycrystals.<sup>[44]</sup>

Similar to the microstructure and crystallographic texture being a direct result of the manufacturing process, the mechanical properties of drawn tungsten wires are linked to its grain structure and orientation. A literature review by Riesch et al.<sup>[73]</sup> showcases the increase in strength of tungsten wires with higher accumulated drawing strain and thus lower diameter. Linked to the decrease in mean grain width (see Figure 6), grain boundary strengthening<sup>[74,75]</sup> as already discussed in literature<sup>[56,76]</sup> can be suspected to contribute to the increase in strength. Similarly, the increase in dislocation density is likely to increase the strength of drawn tungsten wires via Taylor hardening.<sup>[77]</sup> The reduction in area as a measure for ductility obtained in tensile tests performed on drawn tungsten wires with diameters from 63 to 760  $\mu\text{m}$  at  $T > T_{DBT}$  lies around  $(40 \pm 6)\%$ <sup>[76,78,79]</sup> and does not vary significantly with the wire diameter. The evolution of the ultimate tensile strength  $R_m$  increases as a consequence of the reduction of the wire diameter during cold-drawing (see Figure 6).

Detailed discussions of the stress–strain behaviour of as-drawn and annealed tungsten wire can be found in literature (see ref. [51] for pure wires and refs. [73,80] as well as ref. [81] for potassium-doped wires tested at ambient and elevated temperatures, respectively).

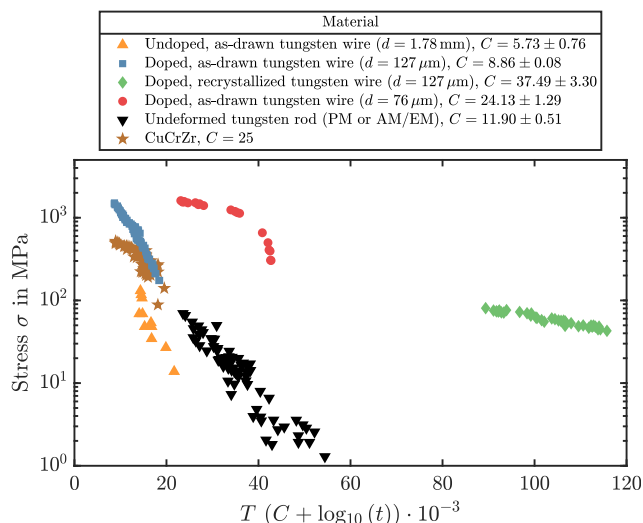


**Figure 7.** Larson–Miller plot (creep stress  $\sigma$  vs. Larson–Miller parameter comprising the temperature  $T$ , the Larson–Miller constant  $C$  and the time to rupture  $t$ ) for different tungsten wires.<sup>[203–206]</sup> The Larson–Miller constant is given in the legend. The data for tungsten wire is compared to creep data of undeformed tungsten produced via powder metallurgy (PM) or arc/electron beam melting (AM/EM)<sup>[207–210]</sup> (black triangles) as well as for Cu–Cr–Zr.<sup>[211]</sup>

Since the application of tungsten wires both as filaments for incandescent lighting as well as reinforcement fibers in advanced composites requires the wires to withstand high stresses at high temperatures for an extended duration, they are required to possess a high resistance against creep deformation. Creep data for doped and undoped tungsten wires with different diameters are shown in **Figure 7** in the form of a Larson–Miller plot.<sup>[82]</sup> It is obvious from **Figure 7** that the creep resistance of tungsten wires is highest for thin, recrystallized wires. This is due to the finer distribution of potassium bubbles leading to a stable microstructure within wires with very high accumulated drawing strain, as already explained previously.

#### 4. The Use of Tungsten Wire in Composites

The exceptional properties of tungsten wires such as the aforementioned high strength and creep resistance even at elevated temperature, makes it attractive for the use as fibrous reinforcements in composites. In this context, both terms, wire reinforcement and fiber reinforcement, are used synonymously. In many cases, the term tungsten fiber is used instead of tungsten wire as soon as it is incorporated into a composite.<sup>[83]</sup>

Although the use for incandescent lighting dominated in the 20<sup>th</sup> century, the use of tungsten wire in combination with a copper matrix became attractive as a model system for metal matrix composites as early as the 1960s. This has been mainly due to the mutual insolubility of W and Cu, the good availability of both constituents (at low costs) and the easy fabrication by liquid melt infiltration.<sup>[6]</sup> Due to their excellent properties the composites have even been considered for applications where high temperature stability, high strength, and high

conductivity are required such as in thrust chambers of rocket engines.<sup>[84]</sup>

Subsequently, the combination of tungsten wire with a wide variety of matrix materials was investigated in NASA studies for use in space applications (for an overview, the reader is referred to ref. [85]). Attempts have been made to utilize the high strength of heavily drawn tungsten wires strength in niobium matrix composites for space nuclear power systems<sup>[86]</sup> as well as in a tungsten based composite material for rocket nozzles.<sup>[87]</sup> Hill et al.<sup>[88]</sup> performed an extensive characterization program on the latter material, which consists of high-strength tungsten wires embedded in a plasma-arc sprayed tungsten matrix. However, although exhibiting good performance in application, material strength was low. Tungsten wire was also proposed as a reinforcement for superalloys in order to increase the application temperature and fatigue resistance and thus achieve longer lifetime. Petrusek et al.<sup>[89]</sup> investigated the use in turbine blades for the high pressure turbo pumps of the Space Shuttle Main Engine. A comprehensive overview of this material group is given in ref. [90].

Using tungsten wire as a reinforcement in composites has once again become a focus for the development of components for the most highly loaded parts of fusion reactors. These components typically consist of a tungsten armor and a copper based heat sink.<sup>[91]</sup> Tungsten wire-reinforcement was proposed to overcome concerns regarding the structural integrity of the baseline heat sink material CuCrZr at high thermal loads and degradation by neutron irradiation which occur, for example, when used as a cooling tube in a mono block concept.<sup>[92]</sup> This development was started within the European integrated Project ExtreMat,<sup>[93]</sup> in which magnetron copper coated wire pieces were consolidated by hot isostatic pressing.<sup>[94]</sup> At the end of this project a first tungsten wire-reinforced Cu tube was tested in high heat flux tests which is the typical qualification test for fusion reactor materials.<sup>[95]</sup> Starting with manual production and engineered interfaces, the next step in developing tungsten fiber-reinforced copper composites ( $W_f/Cu$ ) was the application of textile processes for preform fabrication in combination with liquid melt infiltration.<sup>[96]</sup> These composites exploit the high strength of drawn tungsten wire and thus show a higher strength compared to the CuCrZr baseline material. Even at a testing temperature of 450 °C,  $W_f/Cu$  has a strength of about 500 MPa<sup>[97]</sup> compared to about 300 MPa for pure CuCrZr.<sup>[98]</sup> As the wire features a high temperature stability<sup>[99,100]</sup> the strengthening effect is not impaired during the fabrication process in which a temperature above 1000 °C is reached (Cu melting temperature = 1085 °C<sup>[101]</sup>).

In parallel, ideas of using tungsten as a structural material (see e.g. ref. [102] and references therein) resulted in research on overcoming the inherent brittleness of bulk tungsten below the ductile-to-brittle transition temperature (see chapter 2). Inspired by the work on ceramic fiber-reinforced ceramics<sup>[103]</sup> the use of tungsten wire-reinforced tungsten composites ( $W_f/W$ ) to improve fracture toughness was proposed. In contrast to the aforementioned systems, the reinforcing wire is not mainly intended to increase the strength of the matrix, but rather its resistance to crack propagation. Upon interaction with the wire, mechanisms of energy dissipation are activated in the wake of a growing crack allowing to redistribute stress and thus a reduction of stress peaks at the crack tip. By this, the resistance to crack propagation, i.e., toughness, is increased.<sup>[104]</sup>

A key to the toughening by extrinsic mechanisms are interfacial layers between wire and matrix (hereinafter referred to as interfaces). In order to activate the toughening mechanism, a growing crack has to be deflected when interacting with a wire. This can either be realized by a weak interface<sup>[105]</sup> or a weak matrix region in the vicinity of the wire.<sup>[106]</sup> In the first step, different interfaces were investigated (see ref. [107] and references therein). Successful demonstration tests were carried out on model systems with individual tungsten wire pieces embedded in a tungsten matrix (single fiber sample). In these studies, the significant contribution of the ductile deformation of the wire to the toughening was shown.<sup>[108]</sup> It was also demonstrated that toughening mechanisms remain active even if the wire loses its ductility.<sup>[109]</sup> **Figure 8** shows that all wires break by plastic deformation with necking in a Charpy impact test at room temperature and provides a clear example of the ductility of tungsten wire.<sup>[110,111]</sup> Gietl et al.<sup>[112]</sup> could show that tungsten wire with a diameter of 150  $\mu\text{m}$  incorporated into a tungsten matrix only loses its ductility at a temperature below  $-100\text{ }^\circ\text{C}$ , which is in line with the ductile-to-brittle transition temperature of individual wires with the same diameter (see Figure 4). Tungsten wire features a high specific deformation energy (energy density) in the necking region<sup>[113]</sup> which makes ductile deformation a very effective toughening mechanism.<sup>[109]</sup>

Multi-wire material is fabricated in two ways. Chemical vapour deposition (CVD), utilizing  $\text{WF}_6$  and  $\text{H}_2$ , is used to produce a tungsten matrix around a fibrous preform.<sup>[114]</sup> In a powder metallurgical (PM) process, a mixture of tungsten wire and tungsten powder is consolidated to form the composite material.<sup>[106]</sup> The reinforcement wire is either introduced as a continuous long wire, which is the standard method for CVD composites, or as randomly orientated short wire pieces. Initially, short wire

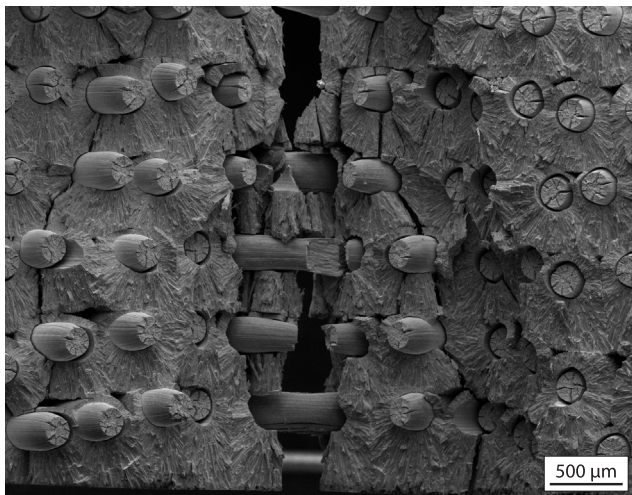


**Figure 8.** Fracture surface of a tungsten fiber-reinforced tungsten composite sample produced by chemical vapour deposition after Charpy impact testing at room temperature: All tungsten wires (diameter 150  $\mu\text{m}$ ) failed in a ductile manner featuring necking and the typical knife-edge fracture surface.<sup>[62]</sup> Details of the fabrication and the mechanical tests are given in ref. [111], where also a high resolution image can be found. Adapted with permission.<sup>[110]</sup> Copyright 2019, Elsevier Ltd.

reinforcement has been used in the PM route, which was later replaced by long wire reinforcement.<sup>[115]</sup> In general long fiber-reinforcement leads to a stronger toughening effect.<sup>[115]</sup> In a further development step, a production method for multi-fiber samples was established and a considerable increase in toughness compared to the non reinforced material was shown.<sup>[116,117]</sup> While composite material produced by powder metallurgy with short fiber reinforcement shows a fracture toughness of about  $20\text{ MPa}\sqrt{\text{m}}$ ,<sup>[118]</sup> long fiber reinforcement leads to values up to  $70\text{ MPa}\sqrt{\text{m}}$ .<sup>[115]</sup> For long fiber composite material produced by chemical vapour deposition values of larger than  $300\text{ MPa}\sqrt{\text{m}}$ <sup>[116]</sup> with a large dependence on fiber volume fraction and sample size (compare e.g., refs. [116,119]) were found. It has to be noted that these values were derived following ASTM399<sup>[120]</sup> standard, which is typically used for homogeneous materials. The authors of these studies therefore note that the test for composite materials does not fulfil all prerequisites of the standard and that values can therefore only give a qualitative idea of the actual fracture toughness. For comparison, the fracture toughness of polycrystalline forged tungsten ranges between 7 and  $15\text{ MPa}\sqrt{\text{m}}$ . All values are for tests at room temperature.

In parallel to processing technology, investigations of the properties of the single wire being the main component of the composite system became focus of research. The emphasis has been on ductility and strength (see e.g., refs. [51,73,80,113,121,122]) as the key capabilities for the composite as well as their temperature stability (see e.g., refs. [81,99,123,124]) (see also chapter 3). While the composites became more mature, their compatibility with the environment expected in a fusion reactor was studied. Mao et al.<sup>[125]</sup> and Kärcher et al.<sup>[126]</sup> demonstrated that erosion and hydrogen retention are acceptable for tungsten wire-reinforced tungsten materials. While tungsten fiber-reinforced copper was already successfully tested in high heat flux experiments,<sup>[127]</sup> first tests have been conducted in the case of tungsten fiber-reinforced tungsten.<sup>[83]</sup> Degradation of material properties by irradiation damage, which is a serious threat for fusion reactor materials, has been shown to be less severe for both individual tungsten wire<sup>[128]</sup> as well as bulk tungsten fiber-reinforced composites.<sup>[97]</sup> A comprehensive overview on the development of tungsten fiber-reinforced composites for fusion reactor applications materials is given in ref. [129] (for  $W_f/W$ ) and refs. [83,130] (for  $W_f/W$  and  $W_f/\text{Cu}$ ).

Attracted by these studies on the wire properties and on tungsten wire composites for fusion applications many development programs for tungsten wire based composites were launched. He et al.<sup>[131]</sup> investigated the use of tungsten wire-reinforced copper as a transition layer between tungsten and CuCrZr. Recently, the use of tungsten wire in combination with a tungsten-zirconium carbide-copper matrix has been investigated.<sup>[132]</sup> The powder metallurgical fabrication of tungsten wire reinforced tungsten was investigated by Zhao et al.<sup>[133]</sup> and Zhang et al.<sup>[134]</sup> The addition of iron to the tungsten powder during this process allows to increase the density but promotes brittle fracture of the tungsten wire.<sup>[135]</sup> In parallel, the recent advances in tungsten fiber-reinforced composite development also puts tungsten wire back into the focus as reinforcement for other matrix materials such as in ceramic<sup>[136]</sup> or polymers.<sup>[137]</sup>

The good compatibility of tungsten with the fusion environment in general and the good availability of tungsten wire have made this material attractive for other applications in plasma-facing components. Terra et al. investigated the concept of free-standing wire pieces embedded in a copper matrix.<sup>[138]</sup> In this concept, which is an advancement of an idea by Matera,<sup>[139]</sup> the free surfaces reduce thermal stresses in the system. Tungsten wire felt and tungsten wire mesh are simultaneously studied as capillary porous systems for liquid metal plasma facing materials.<sup>[140,141]</sup>

#### 4.1. Textile Processing

Manufacturing of composite materials starts with the fabrication of fibrous preforms. Fibrous reinforcements for these preforms can be comprised of continuous or short fibers. While metallic or ceramic reinforcing fibers are often used as monofilaments, glass or carbon reinforcements usually consist of multifilaments. For many years, tungsten monofilaments with a diameter in the range of 100–200  $\mu\text{m}$  were used as reinforcement fibers.<sup>[84,95,104,142]</sup> Fibers with a lower diameter are favoured due to the increased strength (see chapter 3) and flexibility.<sup>[143]</sup> For  $W_f/\text{Cu}$ , monofilaments with diameters as low as 50  $\mu\text{m}$  were utilized.<sup>[96]</sup> However, the smaller the diameter the more challenging the handling becomes. This problem can be solved by utilizing multifilamentary yarns. Several different yarn architectures have been investigated for tungsten wire including enwinding, braiding, and twisting.<sup>[144–146]</sup> Successful use of braided yarns was shown for  $W_f/W$  where they led to better reproducibility of mechanical properties as they allow for a larger fiber volume fraction and a more homogenous fiber distribution due to their large flexibility.<sup>[147]</sup> Recently, upscaling was reported for twisted yarns.<sup>[83]</sup> A number of 14 filaments with a diameter of 16  $\mu\text{m}$  were twisted into two bundles of 7 wires which were then wrapped around each other. In tensile tests, the yarn showed a strength of more than 4 GPa which is very similar to that of the individual wire (see Figure 9). Tungsten wire has been used in hybrid yarns for electromagnetic and radiation shielding in clothes.<sup>[148,149]</sup>

The fibrous preform itself needs to be chosen according to the fabrication technology. For layered fabrication, 2D structures are required (see e.g., ref. [150]). 3D structures are reported for infiltration techniques.<sup>[96]</sup> While in the early development stage of  $W_f/\text{Cu}$  and  $W_f/W$ , manual winding was usually used,<sup>[95,151]</sup> textile techniques are preferred for upscaling. Weaves are investigated as 2D structures for a layered production of  $W_f/W$ .<sup>[111]</sup> Here, a quasi unidirectional reinforcement is achieved by using a large weft wire distance. By utilizing optimised warp wire distances, a significant increase in sample size could be reached for  $W_f/W$  produced by chemical deposition.<sup>[116]</sup> Circular braids have been realized using monofilaments down to a diameter of 50  $\mu\text{m}$ <sup>[144]</sup> as well as multifilamentary yarns.<sup>[83]</sup> In the later case, the textile was optimized to be used in tungsten fiber-reinforced copper tubes. A high braiding angle allows reinforcement in hoop direction. Additionally, axial reinforcement is achieved by introducing yarns in axial direction. Tungsten wire felts produced from wires with a diameter of 50  $\mu\text{m}$  are investigated as capillary porous system for liquid Sn.<sup>[152]</sup>

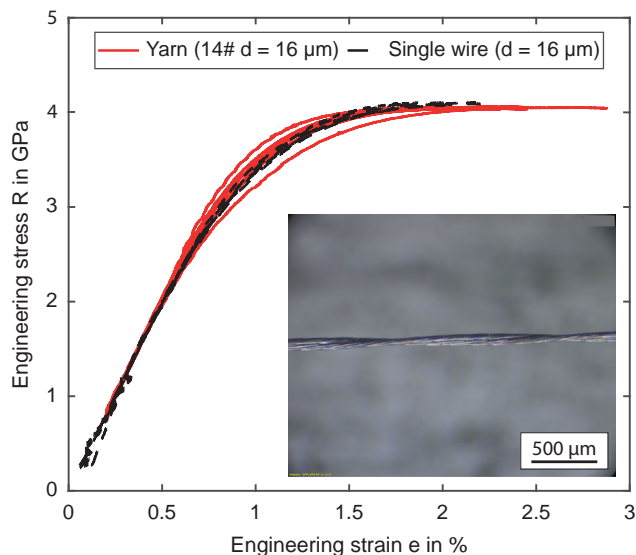


**Figure 9.** Engineering stress–strain curves of a twisted tungsten yarn consisting of (2 times 7) filaments with a diameter of 16  $\mu\text{m}$  (red solid lines) and the individual filament (black dashed line) tested at room temperature. The picture in the right corner shows the yarn in detail. (Reproduced under the terms of the CC BY license.<sup>[83]</sup> Copyright 2024, The Authors. Published by Elsevier Ltd.)

## 5. Discussion

Initially developed as filaments for the lighting industry, thin drawn tungsten wires have found their way into advanced materials for the use in highly loaded components of fusion reactors. The key to this development is the unique combination of high strength and the ability to deform plastically even at low homologous temperatures. Both are linked to the transformation of the wire's microstructure and crystallographic texture during wire drawing. In the following, we will discuss the deformation mechanism of drawn tungsten wires and the wires' potential of their use in composites for the application in nuclear fusion and beyond.

### 5.1. Deformation Mechanism

As already mentioned earlier, a unique feature of drawn tungsten wire is the shift of its ductile-to-brittle transition to lower temperatures after sustained cold-working in the drawing process (see Figure 4). This phenomenon, which is also the basis of the “invention” of ductile tungsten wire by Coolidge (see chapter 2), is also observed in severely plastically deformed (SPD)<sup>[153–156]</sup> and rolled tungsten materials.<sup>[47,68,157–161]</sup> So far, no concise model has been presented in which this “ductilisation” upon cold working could be explained universally. In the following, we present an empirical model that relies on both structure–property relations formulated using current literature and the recent identification of the kink-pair mechanism as rate-controlling deformation mechanism in drawn tungsten wires at  $T > T_{\text{DBT}}$  (see chapter 3).

In drawn tungsten wires, the ductile-to-brittle transition can be described as a competition between two mechanisms, namely



brittle crack growth and dislocation-mediated plastic deformation. For the empirical model, a wire, with an arbitrary flaw, a (micro)crack, an inclusion, a pore, etc., is considered. If the wire is stressed by an external strain rate  $\dot{\epsilon}$ , power is dissipated. The dissipated power per volume  $p$  can be described as follows:

$$p = \frac{dw}{dt} \quad (2)$$

where  $w$  is the dissipated work per volume and  $t$  is the time. On the one hand, work can be dissipated by (incrementally) extending the pre-existing crack, which will eventually lead to a brittle fracture. The associated dissipated work is denominated  $dw_c$ . On the other hand, work can also be dissipated by the generation and/or motion of dislocations. The incremental work for plastic deformation  $dw_{pl}$  can be expressed using the material's strength  $\sigma$  and the plastic strain increment  $\epsilon_{pl}$ :<sup>[60]</sup>

$$dw_{pl} = \sigma d\epsilon_{pl} \quad (3)$$

Whether the material under stress deforms brittle or ductile is determined by the deformation mechanism associated with the lower incremental work. For  $dw_{pl} < dw_c$ , ductile deformation can be expected and vice versa. In order to explain the shift of the ductile-to-brittle transition temperature of tungsten wires upon cold working, the influence of the transformation of the microstructure on the incremental work required for plastic deformation and crack growth has to be analysed, respectively. The impact of changes in the crystallographic texture is most likely negligible since annealing treatments performed by Snow<sup>[162]</sup> led to a dramatic change in the microstructure and mechanical properties of drawn tungsten wires but left the crystallographic texture almost unchanged. Thus, three different microstructural parameters will be discussed below with respect to their evolution with increasing accumulated drawing strain, i.e., decreasing wire diameter, and their corresponding influence on the incremental work that is used to assess the ductile-to-brittle transition.

**Decrease of grain boundary spacing/increase of grain boundary volume:** Foreign atoms like oxygen, nitrogen, carbon, phosphorous and sulfur, which have a low solubility in the bcc lattice, tend to segregate to grain boundaries.<sup>[163,164]</sup> At the grain boundary, the impurities decrease the grain cohesion, requiring less work to split the grain boundary in an intergranular manner.<sup>[165,166]</sup> For a constant impurity content, the decrease in the width of elongated grains and thus the increase in grain boundary area yields an effective dilution of impurities at the grain boundary, improving grain cohesion and increasing the work required for brittle crack growth along the grain boundary. Thus, the decrease in grain width increases  $dw_c$ . Simultaneously, the strength of wires with a smaller grain width increases due to grain boundary strengthening. Thus, a decreased grain boundary spacing also increases  $dw_{pl}$  according to Equation (3).

**Increase of dislocation density:** The cold working during wire drawing increases the dislocation density in tungsten wires (see Figure 6). Thus, the strength of the wire increases due to Taylor hardening. This leads to an increase in the incremental work that is required for the plastic deformation  $dw_{pl}$ .

**Increase in grain length and grain aspect ratio:** As already stated, the grain length and also the grain aspect ratio increase for increasing accumulated drawing strain and thus for decreasing wire diameter.<sup>[48]</sup> Since the fracture toughness of tungsten wires, i.e., their resistance against crack growth, is lowest for intergranular crack propagation,<sup>[167]</sup> cracks that intend to cross the wire transversally from surface to surface first need to follow the highly elongated shape of the grains. A high aspect ratio thus leads to a strong increase in the incremental work  $dw_c$  that is required for brittle fracture by crack propagation. Nikolic et al.<sup>[123]</sup> observed pronounced crack deflection during crack propagation in notched W wire.

In summary, an increase in grain aspect ratio seems to have the most beneficial influence on the ability of a tungsten wire to deform plastically. This result is supported by a study by Pink and Sedlatschek,<sup>[46]</sup> in which they compare the ductile-to-brittle transition temperature of molybdenum materials with different grain aspect ratios. Their study clearly shows that an increase in grain aspect ratio lowers  $T_{DBT}$ . The evolution of  $dw_c$  and  $dw_{pl}$  are depicted schematically as a function of wire diameter in **Figure 10**.

As shown in Figure 10, a critical wire diameter  $d_{crit}(T)$  is defined at a given temperature  $T$  by the intersection of  $dw_{pl}(d)$  and  $dw_c(d)$ . Thicker wires tested at this temperature behave brittle since  $dw_{pl} > dw_c$ , while thinner wires can be deformed to finite plastic strain without fracturing. The influence of the test temperature on the incremental work required for brittle and plastic deformation and thus the ductile-to-brittle transition temperature, is also included in the schematic depiction in Figure 10. The influence of the temperature dependence of the Young's modulus on  $dw_{pl}$  and  $dw_c$  is assumed to be equal for both deformation modes and thus does not change their point of intersection. Hence, the main influence on  $d_{crit}$  is due to the decrease of  $dw_{pl}$  as a direct consequence of the thermally activated nature of

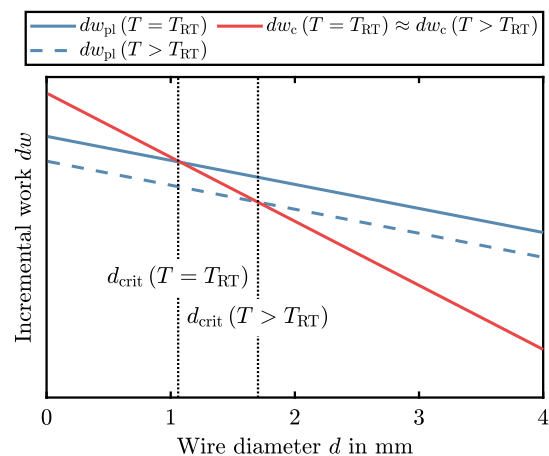


**Figure 10.** Schematic illustration of the dependence of the incremental work for crack propagation  $dw_c$  and for plastic deformation  $dw_{pl}$  on the wire diameter, respectively. The linear dependence was used as first order approximation. The increase of both incremental works is based on the influence of different microstructural parameters, see text. The illustration was set up to fit to the available data on the ductile-to-brittle transition temperatures available in literature, see Figure 4: Plastic behaviour at room temperature  $T_{RT}$  is observed for  $d < d_{crit}(T = T_{RT}) \approx 1\text{ mm}$ .<sup>[5,50]</sup> Higher temperature shifts the critical diameter to higher values, see text.

the kink pair mechanism being the rate-controlling deformation mechanism in drawn tungsten wires at temperatures  $T > T_{DBT}$ . The reader is referred to ref. [168] for an application of the present model on tungsten wires after different treatments (annealing, ion irradiation) as well as rolled tungsten plates and sintered and subsequently thermo-mechanically treated tungsten. While the presented model is in line with theories on the deformation mechanisms of tungsten wires available in literature, it needs to be rationalized by experimental data and robust models based on this experimental data. For this it is essential to use data measured on wires for which both the chemical composition and the process history are known.

## 5.2. Tungsten Wire in Composites for Fusion Application and Beyond

The high strength of tungsten wire allows it to be used as a strengthening element as in  $W_f/Cu$  where the strength of the composite is directly related to the strength of the reinforcement through the rule of mixture.<sup>[6]</sup> If the main intention is toughening, a high strength is beneficial for both elastic bridging of a propagating crack and, less important, for energy dissipation by ductile deformation. While elastic bridging has a quadratic or cubic dependence, ductile deformation has a linear dependence on strength (see ref. [109] and references therein). Although the strength of highly deformed tungsten wire is very high, even in comparison to common reinforcement fiber materials, it has a low specific strength due to its high density (see Table 1). This is not critical for an application in nuclear fusion but could restrict the use of tungsten wire beyond this. Nevertheless, it might still be favorable in applications where weight is no concern and/or if the reinforced matrix is equally dense.<sup>[86]</sup>

If the purpose of fibre-reinforcement is toughening, the ductile deformation during fracture is most beneficial due to the large amount of dissipated energy.<sup>[109]</sup> For this, debonding between wire and matrix is required. The high localized deformation energy density of tungsten wires described earlier enables large energy dissipation even with short debonding lengths.<sup>[113]</sup> This may make tungsten wire attractive for the use in SiC matrix composites, which are also proposed for nuclear applications.<sup>[169]</sup> As a consequence of focused research over many decades SiC reinforced with SiC fibers are believed to have an excellent

**Table 1.** Properties of tungsten wire in comparison to common reinforcement fiber materials. For the comparison, commercially available products were chosen: T300 standard modulus carbon fiber manufactured by Toray carbon fibers America inc.,<sup>[214]</sup> E-glass fiber manufactured by saint-gobain Vetrotex Deutschland GmbH<sup>[215]</sup> and Nicalon (ceramic grade) SiC fiber manufactured by COI Ceramica, inc.<sup>[216,217]</sup>

	Tungsten wire	Carbon	Glass	SiC
Young's modulus in GPa	410	203	73	>340
Strength in GPa	>4 <sup>[73,83]</sup>	3.5	3.4	>2.6
Density in $g\ cm^{-3}$	19.3	1.76	2.6	2.50–2.65
Diameter in $\mu m$	16	7	3–26	14
Fracture	ductile	brittle	brittle	brittle

tolerance against irradiation damage expected in nuclear applications. Although tungsten wire demonstrated a superior irradiation behaviour in first tests<sup>[97,128]</sup> further research is necessary in order to reach the same levels of insight achieved for SiC/SiC composites. The ability of a reinforcing fiber to deform in a ductile manner is moreover of interest for applications beyond nuclear, e.g., in polymer matrix composites. Callens et al.<sup>[170]</sup> showed that the strain to failure of a polymer can be increased up to four times by reinforcing it with ductile steel fibers. As the local deformation energy of tungsten wire is exceeding that of steel wire (compare<sup>[113,171]</sup>) its application in polymers could be attractive.

In the as-drawn state, both undoped and potassium doped tungsten wires show only a moderate decrease in strength during tensile testing up to 600 °C.<sup>[81]</sup> A different behaviour is observed after annealing caused by the different thermal stability of the microstructure: Ductile behaviour accompanied with a decrease in strain hardening capability is observed as long as the elongated grain structure is preserved (see Figure 2). For doped wire with a diameter of 150  $\mu m$  it could be shown that ductility and 70% of the initial strength was retained up to annealing at 2173 K for 0.5 h (see Figure 11).

In contrast to tungsten filaments employed in incandescent lamps, where grain refinement can have a detrimental impact on creep resistance at elevated temperatures, the lower operational temperature range of tungsten wires utilized in fusion applications mitigates the negative influence of small grain sizes on creep strength (see Figure 7). This phenomenon can be illustrated using Ashby deformation maps, wherein the onset of creep is shifted to higher applied stress levels in finer-grained materials, indicating their reduced resistance to withstand creep deformation (see Figure 12). For tungsten wires employed in fusion applications, even with grain sizes as small as 1  $\mu m$ , the contribution of creep deformation is negligible under the prevailing operational conditions. In contrast, for incandescent lamp filaments, comparable creep resistance can only be achieved

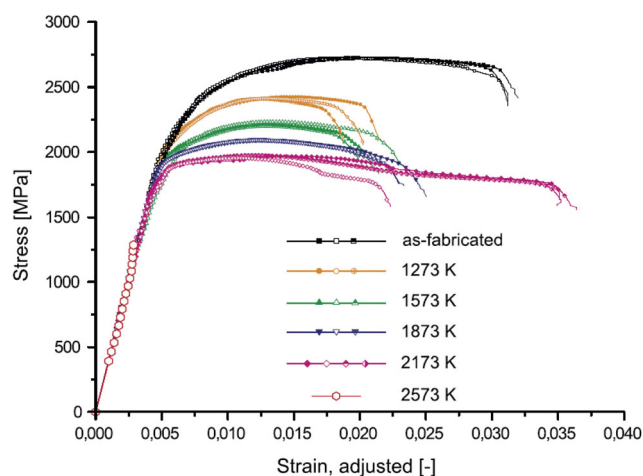


**Figure 11.** Engineering stress–strain curves of as-drawn and annealed doped-tungsten wires with a diameter of 150  $\mu m$  obtained from room temperature tensile tests (taken from<sup>[80]</sup>). The wires were annealed for 0.5 h at the temperatures indicated in the figure legend. Adapted with permission.<sup>[80]</sup> Copyright 2016, IOP Publishing, Ltd.

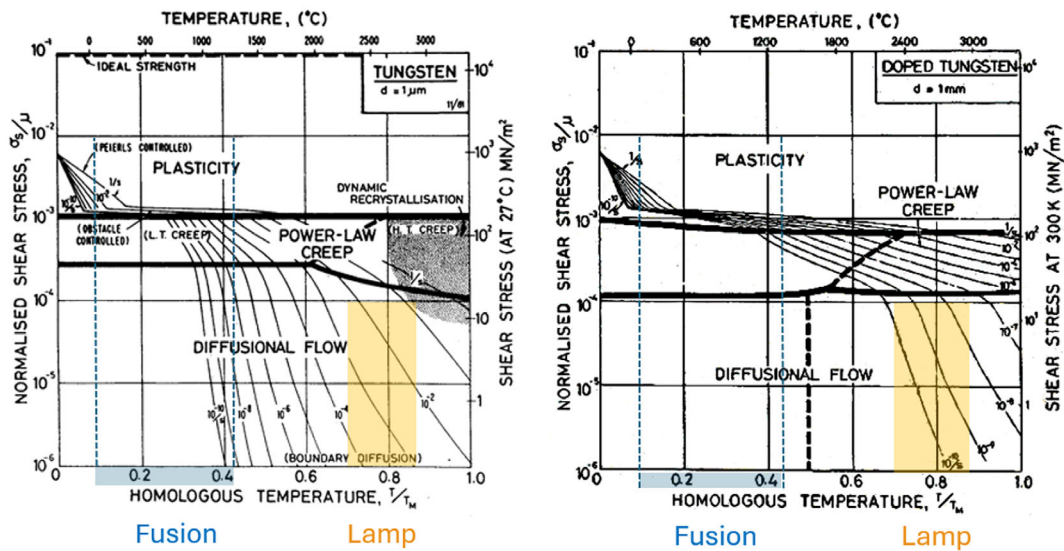


**Figure 12.** Deformation mechanism map of tungsten. Left: Small grained pure tungsten (grain diameter  $d = 1 \mu\text{m}$ ).<sup>[212]</sup> Right: Coarse grained doped tungsten (grain diameter  $d = 1 \text{mm}$ ).<sup>[212]</sup> The colored rectangles indicate the different operating conditions for fusion (blue)<sup>[91]</sup> and incandescent lamps (orange).<sup>[213]</sup> The contour lines for creep rates (labeled by orders of magnitude) demonstrate that even for fine grained tungsten, deformation by creep is negligible for fusion applications, whereas for lamp application comparably low creep rates can only be achieved with doped tungsten wires. Adapted with permission.<sup>[212]</sup> Copyright 1982, Elsevier.

through grain boundary strengthening via doping, as the intrinsic creep resistance of pure tungsten is insufficient to meet the required service life at the elevated operating temperatures.

In the case of  $W_f/Cu$ , the maximum temperature is restricted by the melting point of Cu. Here, the strengthening effect of (in particular doped) tungsten wire used as reinforcement fibre should not be diminished due to annealing phenomena. However, the effect of neutron irradiation (irradiation damage and transmutation) on wire strength and creep stability should be investigated. In the case of  $W_f/W$  the high temperature stability of tungsten wire could allow to increase the maximum operating temperature beyond that of standard materials.<sup>[111]</sup> Open questions are the evolution of strength at temperatures beyond  $600^\circ\text{C}$  and the long time stability of the microstructure within the composite. The maximum annealing time of current studies has been up to 1 h for individual wire.<sup>[80,172]</sup> Longer annealing has been performed in model  $W_f/W$  composite systems (single wire embedded in matrix material).<sup>[173,174]</sup> The studies showed, that besides the effect of longer duration, the interaction with the other composite constituents, i.e., matrix and interface system, has to be taken into account. Radiation-enhanced recrystallisation was reported to be less effective on potassium doped tungsten plates compared to pure W.<sup>[175]</sup> Whether these findings also apply to doped W wire needs to be investigated.

Although, high heat loads are the major load on plasma-facing components, other effects brought about by the within the fusion environment must also be considered, e.g. the effect of neutron irradiation or the interaction of the materials with impurities such as hydrogen. Plasma-facing materials are subjected to high neutron fluxes which can lead to a strong deterioration of mechanical properties.<sup>[176]</sup> As described in chapter 4, thin tungsten wire was resistant against radiation damage in first tests. However, investigations on the role of highly energetic fusion

neutrons and the effect of transmutation are still pending. Hydrogen retention, so far only investigated for wires embedded in a tungsten matrix, seems to be acceptable in the as-fabricated condition. However, as hydrogen retention in tungsten is dominated by defects,<sup>[177]</sup> studies looking into the retention behaviour in the irradiated state are needed to improve understanding. Furthermore, the impact of closed porosity, which is reported for swaged tungsten,<sup>[178]</sup> needs to be studied in more detail. Besides hydrogen, helium produced by the fusion reaction or caused by transmutation is an important species plasma-facing materials are in contact with. Although He loading in a cyclotron did not lead to a detrimental effect on the mechanical properties of hot rolled pure tungsten,<sup>[179]</sup> studies of Das et al.<sup>[180]</sup> showed that synergistic effects, i.e., the interaction of He and irradiation damage, are important. Feichtmayer et al.<sup>[181]</sup> present an interesting method to investigate such effects for tungsten wire and showed first effects on the synergy between mechanical load and irradiation damage. It is also known that tungsten is sensitive to small amounts of impurities which can be beneficial as in the case of potassium (see chapter 2) or detrimental as in the case of carbon or oxygen.<sup>[182]</sup> Müller et al.<sup>[100]</sup> observed embrittlement of tungsten wire during heat treatment in contact with graphite crucibles. A similar finding is reported by Mao et al.<sup>[183]</sup> when investigating the fabrication of  $W_f/W$  by powder metallurgy. As the use of carbon-based materials in plasma-facing components is mostly abandoned due to their high erosion rate and the occurrence of tritium co-deposition,<sup>[184]</sup> direct contact of tungsten with carbon during the use in a fusion reactor environment is unlikely. Nevertheless, due to the high sensitivity towards carbon, utmost care has to be taken in all manufacturing steps before its final use.

As outlined by Riesch et al.<sup>[83]</sup> the design of composites should be based on criteria with respect to the intended

final properties. That means that although the tungsten wire-reinforced composites offer very attractive properties for the use in a fusion reactor, specific applications have to be defined prior to a successful application. A good example is the reinforcement of copper to increase the strength of cooling pipes which was ranked as a risk mitigation material for the next generation of fusion reactors in Europe.<sup>[185]</sup> While the production of tungsten wire textiles is on the brink of industrialization,<sup>[83]</sup> the matrix production procedure is still being optimized for example, by employing galvanic processes.<sup>[186]</sup> The same applies to short fiber-reinforced  $W_f/W$ , where fabrication still takes place in university labs despite a significant upscaling.<sup>[117]</sup>

As tungsten wire was the key component in electric lighting for many decades, there is huge know-how in manufacturing but the once huge production capacities are already decreasing due to a reduced market, e.g. as a consequence of the ban of incandescent light sources in Europe (see e.g. ref. [2] for an overview). In contrast to high performance ceramic fibers, which are mainly produced in the US or Japan,<sup>[187]</sup> tungsten wire is more widely available. The emerging interest in composites for fusion application could open up new markets for drawn tungsten wires. Currently however, the demand of tungsten wire for this application cannot compensate the decreased use for incandescent filaments. However, R&D activities in nuclear fusion technology have recently been ramped up in many countries, which might also provide a strong impetus for the development of tungsten fiber-reinforced composites (see e.g. ref. [188]).

This review focuses on the use of tungsten wire in materials for nuclear fusion application. As outlined above, it might also be attractive to be used in other high-performance composite materials. Many advanced composite materials are being developed for aerospace applications. In this field of application, the high density of tungsten wire will hinder successful application. For example tungsten wire-reinforced FeCrAlY superalloys<sup>[85]</sup> show that the gain in strength by reinforcement is almost completely lost if the composite's normalized strength is compared to the one of the superalloy. The potential of tungsten wire composites could lie in hybrid application e.g., when replacing already used tungsten heavy alloy balance weights for aviation while providing improved structural properties. The same is true when thinking of replacing copper wire in lightning protection.<sup>[189]</sup> When using tungsten wire to reinforce new matrix materials, the chemical compatibility needs to be considered. Whereas the compatibility with a polymer matrix is good<sup>[137]</sup> tungsten wire lost its ductility when combined with a SiC matrix.<sup>[136]</sup>

## 6. Concluding Remarks

The development of a manufacturing process that can produce high-strength, ductile as well as creep-resistant wires from an otherwise brittle tungsten material is unique within the world of metallurgy. This led to the superior qualities of drawn tungsten wires exploited both for incandescent lighting as well as for the development of new and advanced fiber-reinforced composites. The use of drawn tungsten wires as reinforcing fiber can both significantly enhance the high-temperature strength of copper materials as well as bestow considerable fracture

toughness upon an intrinsically brittle tungsten matrix produced via powder metallurgy or chemical vapour deposition. These damage-resilient and reliable composites might pave the way for the break-even of energy production using nuclear fusion. Current efforts are undertaken to qualify tungsten fiber-reinforced composites for the fusion environment as well as optimize the production of these composite materials by for example employing textile techniques.

The development of advanced composite materials reinforced with drawn tungsten wire has the potential to open up new avenues in various industries, including aerospace, energy, and transportation. By leveraging the exceptional mechanical properties and high-temperature stability of drawn tungsten wire, these composites could enable the creation of high-strength and heat-resistant components for the use in extreme environments. The mature manufacturing technology and extensive knowledge base around drawn tungsten wire could facilitate the efficient and cost-effective production of these new composites. The efforts directed towards the use of tungsten wires in these composites have also triggered new research work. Especially strength and ductility, being the key properties for applications in composites became intensive attention. The improved understanding of the mechanical behaviour of tungsten wire especially its low-temperature ductility may also contribute to a better understanding of the mechanical behaviour of other tungsten materials.

Despite the declining demand in lighting, the new application of tungsten wires in composites for fusion reactors can provide drawn tungsten wire with a new lease on life.

## Acknowledgements

The authors want to acknowledge fruitful discussion with Dr.-Ing. Daniel Dicks (University of Bayreuth) on the use of tungsten wire in polymer composites.

Open Access funding enabled and organized by Projekt DEAL.

## Conflict of Interest

The authors declare no conflict of interest.

## Keywords

composites, fiber-reinforcement, lamp filaments, nuclear fusion, tungsten, wire

Received: April 19, 2024

Revised: July 1, 2024

Published online: August 6, 2024

- 
- [1] P. Schade, *Int. J. Refract. Met. Hard Mater.* **2010**, *28*, 648.  
 [2] Z. Koretsky, *Energy Res. Soc. Sci.* **2021**, *82*, 102310.  
 [3] J. Schroder, *Philips Tech. Rev.* **1975**, *35*, 332.  
 [4] W. Schilling, H. Paschedag, *Metallwiss. Tech.* **1960**, *1*, 23.  
 [5] L. L. Seigle, C. D. Dickinson, *Refractory Metals and Alloys: Effect of Mechanical and Structural Variables on the Ductile-Brittle Transition in Refractory Metals*, Interscience, New York, NY **1963**.

- [6] D. L. McDanel, *Tungsten Fiber Reinforced Copper Matrix Composites: A Review*, Nasa Technical Paper 2924, National Aeronautics and Space Administration, Office of Management, Scientific and Technical Information Division, Washington, D.C. **1989**.
- [7] R. Neu, J. Riesch, A. Müller, M. Balden, J. W. Coenen, H. Gietl, T. Höschel, M. Li, S. Wurster, J.-H. You, *Nucl. Mater. Energy* **2017**, *12*, 1308.
- [8] I. Langmuir, J. Orange, *Proc. Am. Inst. Electr. Eng.* **1913**, *32*, 1893.
- [9] E. Lassner, W.-D. Schubert, *ITIA Newsletters* **2005**, p. 2, [https://www.itia.info/wp-content/uploads/2024/05/ITIA\\_Newsletter\\_2005\\_12.pdf](https://www.itia.info/wp-content/uploads/2024/05/ITIA_Newsletter_2005_12.pdf) (accessed: July 2024).
- [10] W. D. Coolidge, *Proc. Am. Inst. Electr. Eng.* **1910**, *29*, 953.
- [11] L. Bartha, E. Lassner, W.-D. Schubert, B. Lux, *Int. J. Refract. Met. Hard Mater.* **1995**, *13*, 1.
- [12] H. Liebhafsky, *William David Coolidge: A Centenarian and His Work*, A Wiley-Interscience Publication, Wiley, New York **1974**.
- [13] A. Pacz, Metal and Its Manufacture, US Patent 1,410,499, **1922**.
- [14] D. B. Snow, *Metall. Trans. A* **1976**, *7*, 783.
- [15] J. Almanstötter, M. Rühle, *Int. J. Refract. Met. Hard Mater.* **1997**, *15*, 295.
- [16] R. Burgin, *Light. Res. Technol.* **1984**, *16*, 61.
- [17] R. C. Koo, *Evidence for Voids in Annealed Doped Tungsten*, Technical Report, Westinghouse Electric Corp., Bloomfield, NJ **1967**.
- [18] G. Das, S. Radcliff, *Journal of Metals*, Vol. 20, Minerals Metals Materials Soc 420 Commonwealth Dr., Warrendale, PA **1968**, p. A43.
- [19] D. Moon, R. Stickler, A. Wolfe, *Sintering of Doped Tungsten Powder*, Technical Report, Westinghouse Research and Development Center, Pittsburgh, **1970**.
- [20] D. Moon, R. Koo, *Metall. Mater. Trans. B* **1971**, *2*, 2115.
- [21] H. Sell, D. Stein, R. Stickler, A. Joshi, E. Berkey, *J. Inst. Met.* **1972**, *100*, 275.
- [22] D. Snow, *Metall. Trans.* **1974**, *5*, 2375.
- [23] K. Kim, G. Welsch, *Mater. Lett.* **1990**, *9*, 295.
- [24] W. M. Haynes, *CRC Handbook of Chemistry and Physics*, CRC Press, Boca Raton **2016**.
- [25] E. Lassner, *Int. J. Refract. Met. Hard Mater.* **1995**, *13*, 35.
- [26] W. Schubert, E. Lassner, *Int. J. Refract. Met. Hard Mater.* **1991**, *10*, 133.
- [27] W. Schubert, E. Lassner, *Int. J. Refract. Met. Hard Mater.* **1991**, *10*, 171.
- [28] B. Bewlay, K. Lou, *Tungsten and Tungsten Alloys*, Minerals, Metals & Materials Society **1991**.
- [29] J. Almanstötter, *Int. J. Refract. Met. Hard Mater.* **2015**, *50*, 290.
- [30] D. Jones, A. Leach, *Powder Metall.* **1979**, *22*, 125.
- [31] J. L. Walter, C. L. Briant, *J. Mater. Res.* **1990**, *5*, 2004.
- [32] J. Almanstötter, *Int. J. Refract. Met. Hard Mater.* **2015**, *50*, 217.
- [33] L. Bartha, P. Harmat, O. Horacsek, T. Grósz, L. Rosta, in *Proc. 4th Int. Conf. Tungsten*, Lake Buena Vista, FL, November **1997**, pp. 203–210.
- [34] B. Bewlay, N. Lewis, K. Lou, *Metall. Trans. A* **1992**, *23*, 121.
- [35] C. Briant, F. Zaverl, E. Hall, *Mater. Sci. Technol.* **1991**, *7*, 923.
- [36] K. Tanoue, O. Nakano, H. Mori, H. Matsuda, *J. Jpn. Inst. Met.* **1984**, *48*, 618.
- [37] O. Horacsek, C. L. Tóth, A. Nagy, *Int. J. Refract. Met. Hard Mater.* **1998**, *16*, 51.
- [38] H. Warlimont, G. Necker, H. Schultz, *Int. J. Mater. Res.* **1975**, *66*, 279.
- [39] H. P. Stüwe, *Metall. Trans. A* **1986**, *17*, 1455.
- [40] P. K. Wright, *Metall. Trans. A* **1978**, *9*, 955.
- [41] Night Breaker 200 – Brightest OSRAM Halogen Light, Product Family Datasheet, [https://www.osram.de/ecat/NIGHT%20BREAKER%20200-Halogen%20headlight%20lamps-Car%20lighting-Automotive/tr/en/GPS01\\_3495633/](https://www.osram.de/ecat/NIGHT%20BREAKER%20200-Halogen%20headlight%20lamps-Car%20lighting-Automotive/tr/en/GPS01_3495633/) (accessed: July 2024).
- [42] W. D. Coolidge, US Patent 1,082,933, **1913**.
- [43] U.S. District Court for the District of Delaware, 17 f.2d 90, General Electric Co. v. De Forest Radio Co., no. 561, <https://law.justia.com/cases/federal/district-courts/F2/17/90/1487908/> (accessed: July 2024).
- [44] A. Giannattasio, S. G. Roberts, *Philos. Mag.* **2007**, *87*, 2589.
- [45] E. Gaganidze, A. Chauhan, J. Aktaa, *Fusion Eng. Des.* **2022**, *184*, 113300.
- [46] E. Pink, K. Sedlatschek, *Metall* **1969**, *23*, 1249.
- [47] C. Bonnekoh, U. Jäntsch, J. Hoffmann, H. Leiste, A. Hartmaier, D. Weygand, A. Hoffmann, J. Reiser, *Int. J. Refract. Met. Hard Mater.* **2019**, *78*, 146.
- [48] *The Metallurgy of Doped/Non-Sag Tungsten*, 1st ed. (Eds: E. Pink, L. Bartha), Elsevier Applied Science, Essex **1989**.
- [49] J. F. Peck, D. A. Thomas, *Trans. Metall. Soc. AIME* **1961**, *221*, 1240.
- [50] R. Eck, *Metall* **1979**, *33*, 819.
- [51] P. Zhao, J. Riesch, T. Höschel, J. Almanstötter, M. Balden, J. W. Coenen, R. Himml, W. Pantleon, U. von Toussaint, R. Neu, *Int. J. Refract. Met. Hard Mater.* **2017**, *68*, 29.
- [52] X. Zhang, Q. Yan, S. Lang, M. Xia, C. Ge, *J. Nucl. Mater.* **2016**, *468*, 339.
- [53] J. A. Mullendore, in *The Metallurgy of Doped/Non-Sag Tungsten* (Eds: E. Pink, L. Bartha), Elsevier Applied Science, Essex **1989**, pp. 61–82, ISBN 1-85166-390-8.
- [54] S. Leber, *Transaction of the Metallurgical Society of AIME* **1965**, *233*, 953.
- [55] W. J. Hosford Jr., *Trans. Metall. Soc. AIME* **1964**, *230*, 12.
- [56] E. S. Meieran, D. A. Thomas, *Trans. Metall. Soc. AIME* **1965**, *223*, 937.
- [57] J. L. Walter, E. F. Koch, *J. Mater. Sci.* **1991**, *26*, 505.
- [58] M. R. Ripoll, J. Očenášek, *Eng. Fract. Mech.* **2009**, *76*, 1485.
- [59] P. Van Houtte, in *Proc. 7. Int. Conf. Texture of Materials* (Ed: C. M. Brakman), Netherlands Society for Materials, Zwijndrecht **1984**, pp. 7–23.
- [60] W. F. Hosford, *The Mechanics of Crystals and Textured Polycrystals*, Oxford University Press, New York and Oxford **1993**.
- [61] S. Zhou, J. Yang, Y. Zhang, P. Zhang, Z. Nie, *J. Mater. Res. Technol.* **2021**, *15*, 6434.
- [62] S. Leber, J. Tavernelli, D. D. White, R. F. Hehemann, *J. Less-Common Met.* **1976**, *48*, 119.
- [63] T. Millner, L. Varga, B. Verö, *Z. Metallkd.* **1972**, *63*, 754.
- [64] H. Schultz, *Z. Naturkd.* **1959**, *14*, 361.
- [65] M. Fuhr, T. Höschel, J. Riesch, M. Boleininger, J. Almanstötter, W. Pantleon, R. Neu, *Philos. Mag.* **2023**, *103*, 1029.
- [66] A. Seeger, *London, Edinburgh Dublin Philos. Mag. J. Sci.* **1954**, *45*, 771.
- [67] S. W. Bonk, *Ph.D. Thesis*, Karlsruher Institut für Technologie, Karlsruhe, **2018**.
- [68] C. Bonnekoh, J. Reiser, A. Hartmaier, S. Bonk, A. Hoffmann, M. Rieth, *J. Mater. Sci.* **2020**, *55*, 12314.
- [69] D. Kiener, R. Fritz, M. Alfreider, A. Leitner, R. Pippan, V. Maier-Kiener, *Acta Mater.* **2019**, *166*, 687.
- [70] J. Kappacher, A. Leitner, D. Kiener, H. Clemens, V. Maier-Kiener, *Mater. Des.* **2020**, *189*, 108499.
- [71] D. Brunner, *Mater. Trans.* **2000**, *41*, 152.
- [72] D. Brunner, V. Glebovsky, *Mater. Lett.* **2000**, *44*, 144.
- [73] J. Riesch, A. Feichtmayer, M. Fuhr, J. Almanstötter, J. W. Coenen, H. Gietl, T. Höschel, C. Linsmeier, R. Neu, *Phys. Scr.* **2017**, *T170*, 014032.
- [74] E. O. Hall, *Proc. Phys. Soc. London, Sect. B* **1951**, *64*, 747.
- [75] N. J. Petch, *J. Iron Steel Inst.* **1953**, *174*, 25.
- [76] D. A. Thomas, E. S. Comerford, E. S. Meieran, J. F. Peck, F. T. J. Smith, in *Substructure and Mechanical Properties of Refractory Metals* (Ed: I. Perlmutter), Defense Documentation Center for Scientific and Technical Information, Alexandria, Virginia **1963**, pp. 74–123.
- [77] G. I. Taylor, *Proc. R. Soc. London, Ser. A* **1934**, *145*, 362.
- [78] D. Lee, *Metall. Trans. A* **1975**, *6*, 2083.

- [79] B. S. Lement, M. Cohen, E. M. Passmore, K. Kreder, I. Vilks, in *Substructure and Mechanical Properties of Refractory Metals* (Eds: I. Perlmutter), Defense Documentation Center for Scientific and Technical Information, Alexandria, Virginia **1963**.
- [80] J. Riesch, Y. Han, J. Almanstötter, J. W. Coenen, T. Hösch, B. Jasper, P. Zhao, C. Linsmeier, R. Neu, *Phys. Scr.* **2016**, T167, 014006.
- [81] D. Terentyev, J. Riesch, S. Lebediev, A. Bakaeva, J. W. Coenen, *Int. J. Refract. Met. Hard Mater.* **2017**, 66, 127.
- [82] F. R. Larson, J. Miller, *Trans. ASME* **1952**, 74, 765.
- [83] J. Riesch, A. von Müller, Y. Mao, J. W. Coenen, B. Böswirth, S. Elgeti, M. Fuhr, H. Greuner, T. Hösch, K. Hunger, P. Junghanns, A. Lau, S. Roccella, L. Vanlitsenburgh, J.-H. You, C. Linsmeier, R. Neu, *Nucl. Mater. Energy* **2024**, 38, 101591.
- [84] J. M. Kazaroff, R. S. Jankovsky, Cyclic Hot Firing Results of Tungsten-Wire-Reinforced, Copper-Lined Thrust Chambers, <https://ntrs.nasa.gov/citations/19920022005> (accessed: July 2024).
- [85] J. Doychak, *JOM* **1992**, 44, 46.
- [86] R. H. Titran, T. L. Grobstein, *JOM* **1990**, 42, 8.
- [87] T. Greening, E. Eppinger, S. Jacobs, in *3rd Solid Propulsion Conf.*, American Institute of Aeronautics and Astronautics, Reston, Virginia **1968**.
- [88] J. G. Hill, F. L. Banta, Characterization of Wire-Wound Tungsten Composite, <https://apps.dtic.mil/sti/citations/AD0743978> (accessed: July 2024).
- [89] D. W. Petrusek, J. R. Stephens, *Fiber-Reinforced Superalloys for Rocket Engines*, **1988**.
- [90] D. W. Petrusek, R. A. Signorelli, in *Proc. 5th Annual Conf. Composites and Advanced Ceramic Materials: Ceramic Engineering and Science Proc., Volume 2, Issue 7/8, Volume 2 of Ceramic Engineering and Science Proc.* (Ed: W. J. Smothers), John Wiley & Sons, Inc., Hoboken, NJ **1981**, pp. 739–786, ISBN 9780470291092.
- [91] J. W. Coenen, S. Antusch, M. Aumann, W. Biel, J. Du, J. Engels, S. Heuer, A. Houben, T. Hoeschen, B. Jasper, F. Koch, J. Linke, A. Litnovsky, Y. Mao, R. Neu, G. Pintsuk, J. Riesch, M. Rasinski, J. Reiser, M. Rieth, A. Terra, B. Unterberg, T. Weber, T. Wegener, J.-H. You, C. Linsmeier, *Phys. Scr.* **2016**, T167, 014002.
- [92] J.-H. You, *Nucl. Mater. Energy* **2015**, 5, 7.
- [93] ExtreMat IP: New Materials for Extreme Environments, <https://cordis.europa.eu/project/id/500253/reporting> (accessed: July 2024).
- [94] P. W. M. Peters, J. Hempenmacher, H. Schurmann, *Materialwiss. Werkstofftech.* **2007**, 38, 755.
- [95] A. Herrmann, H. Greuner, M. Balden, H. Bolt, *Fusion Eng. Des.* **2011**, 86, 27.
- [96] A. Müller, D. Ewert, A. Galatanu, M. Milwich, R. Neu, J. Y. Pastor, U. Siefken, E. Tejado, J. H. You, *Fusion Eng. Des.* **2017**, 124, 455.
- [97] D. Terentyev, M. Rieth, G. Pintsuk, A. von Müller, S. Antusch, A. Zinovev, A. Bakaev, K. Poleshchuk, G. Aiello, *J. Nucl. Mater.* **2023**, 584, 154587.
- [98] V. R. Barabash, G. M. Kalinin, S. A. Fabritsiev, S. J. Zinkle, *J. Nucl. Mater.* **2011**, 417, 904.
- [99] D. Terentyev, J. Riesch, S. Lebediev, T. Khvan, A. Dubinko, A. Bakaeva, *Int. J. Refract. Met. Hard Mater.* **2018**, 76, 226.
- [100] A. V. Müller, M. Ilg, H. Gietl, T. Hösch, R. Neu, G. Pintsuk, J. Riesch, U. Siefken, J. H. You, *Nucl. Mater. Energy* **2018**, 16, 163.
- [101] X. Liu, X. Xiong, in *Encyclopedia of Geochemistry, Encyclopedia of Earth Sciences Series* (Ed: W. M. White), Springer International Publishing, Cham **2018**, pp. 303–305, ISBN 978-3-319-39311-7.
- [102] J.-H. You, *Nucl. Fusion* **2015**, 55, 113026.
- [103] A. G. Evans, *J. Am. Ceram. Soc.* **1990**, 73, 187.
- [104] J. Riesch, T. Hösch, C. Linsmeier, S. Wurster, J.-H. You, *Phys. Scr.* **2014**, T159, 014031.
- [105] J. Du, T. Hösch, M. Rasinski, S. Wurster, W. Grosinger, J.-H. You, *Compos. Sci. Technol.* **2010**, 70, 1482.
- [106] Y. Mao, J. Coenen, S. Sistla, C. Liu, A. Terra, X. Tan, J. Riesch, T. Hoeschen, Y. Wu, C. Broeckmann, C. Linsmeier, *Mater. Sci. Eng., A* **2021**, 817, 141361.
- [107] J. Du, J.-H. You, T. Hösch, *J. Mater. Sci.* **2012**, 47, 4706.
- [108] J. Riesch, J.-Y. Buffiere, T. Hösch, M. Di Michiel, M. Scheel, C. Linsmeier, J.-H. You, *Acta Mater.* **2013**, 61, 7060.
- [109] J. Riesch, J.-Y. Buffiere, T. Hösch, M. Scheel, C. Linsmeier, J.-H. You, *Nucl. Mater. Energy* **2018**, 15, 1.
- [110] J. d'Angelo, J. Riesch, Y. Zayachuk, R. Thomas, *J. Nucl. Mater.* **2019**, 519, 332.
- [111] J. Riesch, M. Aumann, J. W. Coenen, H. Gietl, G. Holzner, T. Hösch, P. Huber, M. Li, C. Linsmeier, R. Neu, *Nucl. Mater. Energy* **2016**, 9, 75.
- [112] H. Gietl, J. Riesch, T. Hösch, M. Rieth, J. W. Coenen, R. Neu, *Mater. Lett.* **2022**, 311, 131526.
- [113] J. Riesch, J. Almanstötter, J. W. Coenen, M. Fuhr, H. Gietl, Y. Han, T. Hösch, C. Linsmeier, N. Travitzky, P. Zhao, R. Neu, *IOP Conf. Ser.: Mater. Sci. Eng.* **2016**, 139, 012043.
- [114] L. Raumann, J. W. Coenen, J. Riesch, Y. Mao, D. Schwalenberg, T. Wegener, H. Gietl, T. Hösch, C. Linsmeier, O. Guillon, *Nucl. Mater. Energy* **2021**, 28, 101048.
- [115] Y. Mao, J. W. Coenen, C. Liu, A. Terra, X. Tan, J. Riesch, T. Hösch, Y. Wu, C. Broeckmann, C. Linsmeier, *J. Nucl. Eng.* **2022**, 3, 446.
- [116] D. Schwalenberg, J. W. Coenen, J. Riesch, T. Hoeschen, Y. Mao, A. Lau, H. Gietl, L. Raumann, P. Huber, C. Linsmeier, R. Neu, *J. Nucl. Eng.* **2022**, 3, 306.
- [117] J. W. Coenen, V. Y. S. Lee, Y. Mao, A. Morrison, D. Dorow-Gerspach, X. Tan, A. Terra, Y. Wu, C. Linsmeier, *Adv. Eng. Mater.* **2023**, 25, 19.
- [118] Y. Mao, J. W. Coenen, J. Riesch, S. Sistla, J. Almanstötter, J. Reiser, A. Terra, C. Chen, Y. Wu, L. Raumann, T. Hösch, H. Gietl, R. Neu, C. Linsmeier, C. Broeckmann, *Nucl. Fusion* **2019**, 59, 086034.
- [119] H. Gietl, S. Olbrich, J. Riesch, G. Holzner, T. Hösch, J. W. Coenen, R. Neu, *Eng. Fract. Mech.* **2020**, 232, 107011.
- [120] E08 Committee, E399 - 90: Test Method for Linear-Elastic Plane-Strain Fracture Toughness of Metallic Materials.
- [121] D. Terentyev, J. Riesch, S. Lebediev, T. Khvan, A. Zinovev, M. Rasiński, A. Dubinko, J. W. Coenen, *Int. J. Refract. Met. Hard Mater.* **2018**, 73, 38.
- [122] D. Terentyev, A. Dubinko, J. Riesch, S. Lebediev, I. Volkov, E. E. Zhurkin, *Int. J. Refract. Met. Hard Mater.* **2020**, 86, 105094.
- [123] V. Nikolić, J. Riesch, M. J. Pfeifenberger, R. Pippin, *Mater. Sci. Eng., A* **2018**, 737, 434.
- [124] D. Terentyev, J. Riesch, A. Dubinko, T. Khvan, E. E. Zhurkin, *Fusion Eng. Des.* **2019**, 146, 991.
- [125] Y. Mao, J. W. Coenen, A. Terra, L. Gao, A. Kreter, M. Wirtz, C. Liu, C. Chen, J. Riesch, Y. Wu, C. Broeckmann, C. Linsmeier, *Nucl. Fusion* **2022**, 62, 106029.
- [126] A. Kärcher, J. Riesch, P. Almanstötter, A. Manhard, M. Balden, J. W. Coenen, K. Hunger, H. Maier, L. Raumann, D. Schwalenberg, R. Neu, *Nucl. Mater. Energy* **2021**, 27, 100972.
- [127] A. V. Müller, B. Böswirth, V. Cerri, H. Greuner, R. Neu, U. Siefken, E. Visca, J. H. You, *Phys. Scr.* **2020**, T171, 014015.
- [128] J. Riesch, A. Feichtmayer, J. W. Coenen, B. Curzadd, H. Gietl, T. Hösch, A. Manhard, T. Schwarz-Selinger, R. Neu, *Nucl. Mater. Energy* **2022**, 30, 101093.
- [129] J. W. Coenen, *Adv. Eng. Mater.* **2020**, 22, 1901376.
- [130] C. Linsmeier, M. Rieth, J. Aktaa, T. Chikada, A. Hoffmann, J. Hoffmann, A. Houben, H. Kurishita, X. Jin, M. Li, A. Litnovsky, S. Matsuo, A. von Mueller, V. Nikolic, T. Palacios, R. Pippin, D. Qu, J. Reiser, J. Riesch, T. Shikama, R. Stieglitz, T. Weber, S. Wurster, J.-H. You, Z. Zhou, *Nucl. Fusion* **2017**, 57, 9.

- [131] G. He, K. Xu, S. Guo, X. Qian, Z. Yang, G. Liu, J. Li, J. Nucl. Mater. **2014**, 455, 225.
- [132] D. Wang, K. Xu, B. Wei, X. Ding, S. Ran, JOM **2022**, 74, 4307.
- [133] S. X. Zhao, F. Liu, S. G. Qin, J. P. Song, G.-N. Luo, Fusion Sci. Technol. **2013**, 64, 225.
- [134] L. Zhang, Y. Jiang, Q. Fang, Z. Xie, S. Miao, L. Zeng, T. Zhang, X. Wang, C. Liu, Front. Mater. Sci. **2017**, 11, 190.
- [135] S. Chen, Z. Jiang, J. Yang, Z. Ye, J. Huang, Int. J. Refract. Met. Hard Mater. **2023**, 116, 106369.
- [136] B. Mainzer, C. Lin, M. Frieß, R. Riedel, J. Riesch, A. Feichtmayer, M. Fuhr, J. Almanstötter, D. Koch, J. Eur. Ceram. Soc. **2021**, 41, 3030.
- [137] D. Dickes, S. Maidl, J. Riesch, R. Neu, K. Drechler **2024**.
- [138] A. Terra, G. Sergienko, M. Tokar, D. Borodin, T. Dittmar, A. Huber, A. Kreter, Y. Martynova, S. Möller, M. Rasiński, M. Wirtz, T. Loewenhoff, D. Dorow-Gerspach, Y. Yuan, S. Brezinsek, B. Unterberg, C. Linsmeier, Nucl. Mater. Energy **2019**, 19, 7.
- [139] R. Matera, Diverter-Collector for a Tokamak Nuclear Fusion Reactor: European Patent, <https://patents.google.com/patent/EP0280940B1/en> (accessed: July 2024).
- [140] T. W. Morgan, A. Vertkov, K. Bystrov, I. Lyublinski, J. W. Genuit, G. Mazzitelli, Nucl. Mater. Energy **2017**, 12, 210.
- [141] Z.-B. Ye, X.-C. Ma, P.-N. He, Z.-J. Wang, C. Yang, B. Chen, J.-J. Chen, J.-J. Wei, K. Zhang, F.-J. Gou, Tungsten **2020**, 2, 94.
- [142] J. L. Yuen, D. W. Petrasek, J. Compos. Technol. Res. **1994**, 16, 343.
- [143] K. K. Chawla, Composite Materials, Springer, New York, NY **2012**.
- [144] H. Gietl, A. V. Müller, J. W. Coenen, M. Decius, D. Ewert, T. Höschen, P. Huber, M. Milwich, J. Riesch, R. Neu, J. Compos. Mater. **2018**, 52, 3875.
- [145] J. W. Coenen, M. Treitz, H. Gietl, P. Huber, T. Hoeschen, L. Raumann, D. Schwalenberg, Y. Mao, J. Riesch, A. Terra, C. Broeckmann, O. Guillon, C. Linsmeier, R. Neu, Phys. Scr. **2020**, T171, 014061.
- [146] J. W. Coenen, P. Huber, A. Lau, L. Raumann, D. Schwalenberg, Y. Mao, J. Riesch, A. Terra, C. Linsmeier, R. Neu, Phys. Scr. **2021**, 96, 124063.
- [147] A. Lau, J. W. Coenen, D. Schwalenberg, Y. Mao, T. Höschen, J. Riesch, L. Raumann, M. Treitz, H. Gietl, A. Terra, B. Göhls, C. Linsmeier, K. Theis-Bröhl, J. Gonzalez-Julian, J. Nucl. Eng. **2023**, 4, 375.
- [148] A. Telli, O. Babaarslan, S. Karaduman, Adv. Res. Text. Eng. **2017**, 2, 1013.
- [149] S.-C. Kim, J. S. Son, Sci. Rep. **2021**, 11, 3676.
- [150] H. Gietl, J. Riesch, J. W. Coenen, T. Höschen, R. Neu, Fusion Eng. Des. **2019**, 146, 1426.
- [151] J. Riesch, T. Höschen, A. Galatanu, J.-H. You, in Proc. 18th Int. Conf. Composite Materials **2011**, <https://iccm-central.org/Proceedings/ICCM18proceedings/papers/M29-3-IF0239.pdf> (accessed: July 2024).
- [152] A. Vertkov, I. Lyublinski, M. Zharkov, G. Mazzitelli, M. L. Apicella, M. Iafrazi, Fusion Eng. Des. **2017**, 117, 130.
- [153] H. Yuan, Y. Zhang, A. V. Ganeev, J. T. Wang, I. V. Alexandrov, Mater. Sci. Forum **2010**, 667, 701.
- [154] I. V. Alexandrov, G. I. Raab, V. U. Kazhyanov, L. O. Sheastakova, R. Z. Valiev, R. J. Dowding, Ultrafine Grained Materials II, Wiley **2002**, pp. 199–207, ISBN 9781118804537.
- [155] Z. S. Levin, K. T. Hartwig, Mater. Sci. Eng., A **2017**, 707, 602.
- [156] K. Xue, Y. Guo, J. Shi, X. Wei, P. Li, Mater. Sci. Eng., A **2022**, 832, 142513.
- [157] J. Reiser, Dissertation, Karlsruher Institut für Technologie, Karlsruhe, **2012**.
- [158] S. Bonk, J. Reiser, J. Hoffmann, A. Hoffmann, Int. J. Refract. Met. Hard Mater. **2016**, 60, 92.
- [159] S. Bonk, J. Hoffmann, A. Hoffmann, J. Reiser, Int. J. Refract. Met. Hard Mater. **2018**, 70, 124.
- [160] C. Bonnekoh, A. Hoffmann, J. Reiser, Int. J. Refract. Met. Hard Mater. **2018**, 71, 181.
- [161] J. Reiser, J. Hoffmann, U. Jäntsche, M. Klimenkov, S. Bonk, C. Bonnekoh, M. Rieth, A. Hoffmann, T. Mrotzek, Int. J. Refract. Met. Hard Mater. **2016**, 54, 351.
- [162] D. B. Snow, Metall. Trans. A **1979**, 10, 815.
- [163] K. Leitner, Dissertation, Montanuniversität Leoben, Leoben, **2017**.
- [164] B. Gludovatz, S. Wurster, T. Weingärtner, A. Hoffmann, R. Pippan, Philos. Mag. **2011**, 91, 3006.
- [165] C. Ren, Z. Fang, M. Koopman, B. Butler, J. Paramore, S. Middlemas, Int. J. Refract. Met. Hard Mater. **2018**, 75, 170.
- [166] A. M. Russell, K. L. Lee, Structure-Property Relations in Nonferrous Metals, Wiley-Interscience, Hoboken, NJ **2005**.
- [167] M. J. Pfeifenberger, V. Nikolić, S. Žák, A. Hohenwarther, R. Pippan, Acta Mater. **2019**, 176, 330.
- [168] M. Fuhr, Ph.D. Thesis, Technische Universität München, München **2024**, <https://mediatum.ub.tum.de/?id=1709412>.
- [169] T. Noda, in Handbook of Advanced Ceramics and Composites (Eds: Y. Mahajan, J. Roy), Springer International Publishing, Cham **2019**, pp. 1–26, ISBN 978-3-319-73255-8.
- [170] M. G. Callens, L. Gorbatikh, I. Verpoest, Composites, Part A **2014**, 61, 235.
- [171] S. R. Pemberton, E. K. Oberg, J. Dean, D. Tsarouchas, A. E. Markaki, L. Marston, T. W. Clyne, Compos. Sci. Technol. **2011**, 71, 266.
- [172] V. Nikolić, J. Riesch, R. Pippan, Mater. Sci. Eng., A **2018**, 737, 422.
- [173] U. M. Ciucani, L. Haus, H. Gietl, J. Riesch, W. Pantleon, J. Nucl. Mater. **2021**, 543, 152579.
- [174] D. A. H. Wartacz, J. Riesch, K. Pantleon, W. Pantleon, J. Phys.: Conf. Ser. **2023**, 2635, 012034.
- [175] H. Gietl, T. Koyanagi, X. Hu, M. Fukuda, A. Hasegawa, Y. Katoh, J. Alloys Compd. **2022**, 901, 163419.
- [176] E. Gaganidze, A. Chauhan, H.-C. Schneider, D. Terentyev, B. Rossaert, J. Aktaa, J. Nucl. Mater. **2021**, 556, 153200.
- [177] T. Schwarz-Selinger, Mater. Res. Express **2023**, 10, 102002.
- [178] A. Hoffmann, I. Wesemann, Int. J. Powder Metall. **2011**, 47, 11.
- [179] T. Miyazawa, T. Hwang, K. Tsuchida, T. Hattori, M. Fukuda, S. Nogami, A. Hasegawa, Nucl. Mater. Energy **2018**, 15, 154.
- [180] S. Das, H. Yu, E. Tarleton, F. Hofmann, Sci. Rep. **2019**, 9, 18354.
- [181] A. Feichtmayer, M. Boleininger, J. Riesch, D. R. Mason, L. Reali, T. Höschen, M. Fuhr, T. Schwarz-Selinger, R. Neu, S. L. Dudarev, Fast Low-Temperature Irradiation Creep Driven by Athermal Defect Dynamics.
- [182] J. R. Stephens, Effects of Interstitial Impurities on the Low-Temperature Tensile Properties of Tungsten, <https://apps.dtic.mil/sti/pdfs/ADA396979.pdf> (accessed: July 2024).
- [183] Y. Mao, C. Chen, J. W. Coenen, J. Riesch, S. Sistla, J. Almanstötter, A. Terra, Y. Wu, L. Raumann, T. Höschen, H. Gietl, R. Neu, C. Linsmeier, C. Broeckmann, Fusion Eng. Des. **2019**, 145, 18.
- [184] J. Roth, E. Tsitrone, A. Loarte, T. Loarer, G. Counsell, R. Neu, V. Philipps, S. Brezinsek, M. Lehnen, P. Coad, C. Grisolia, K. Schmid, K. Krieger, A. Kallenbach, B. Lipschultz, R. Doerner, R. Causey, V. Alimov, W. Shu, O. Ogorodnikova, A. Kirschner, G. Federici, A. Kukushkin, J. Nucl. Mater. **2009**, 390, 1.
- [185] J. H. You, E. Visca, T. Barrett, B. Böswirth, F. Crescenzi, F. Domptail, G. Dose, M. Fursdon, F. Gallay, H. Greuner, K. Hunger, A. Lukenskas, A. Müller, M. Richou, S. Roccella, C. Vorpahl, K. Zhang, J. Nucl. Mater. **2021**, 544, 152670.
- [186] P. Junghanns, M. Busch, A. V. Müller, S. Roccella, K. Hunger, J.-H. You, R. Neu, J. Riesch, J. Boscaro, Fusion Eng. Des. **2024**, 201, 114268.
- [187] S. Yilmaz, M. Theodore, S. Ozcan, Composites, Part B **2024**, 269, 111101.
- [188] IAEA World Fusion Outlook 2023, International Atomic Energy Agency, Vienna **2023**, <https://www.iaea.org/publications/15524/iaea-world-fusion-outlook-2023>.

- [189] M. Gagné, D. Theriault, in *Progress in Aerospace Sciences*, Vol. 64, Elsevier **2014**, pp. 1–16. <https://doi.org/10.1016/j.paerosci.2013.07.002>.
- [190] S. W. Yih, C. T. Wang, *Tungsten: Sources, Metallurgy, Properties and Applications*, Plenum Press, New York and London **1979**.
- [191] C. Agte, J. Vacek, *Wolfram Und Molybdän*, Akademie Verlag, Berlin **1959**.
- [192] P. Schade, *Int. J. Refract. Met. Hard Mater.* **2006**, 24, 332.
- [193] C. L. Briant, O. Horacsek, K. Horacsek, *Metall. Trans. A* **1993**, 24, 843.
- [194] L. Uray, A. Sulyok, P. Tekula-Buxbaum, *High Temp. Mater. Process.* **2005**, 24, 5.
- [195] L. Bartha, E. Lassner, W.-D. Schubert, B. Lux, *The Chemistry of Non-Sag Tungsten*, 1st ed., Pergamon, Oxford **1995**.
- [196] A. Szökefalvi-Nagy, G. Radnoczi, I. Gaal, *Mater. Sci. Eng.* **1987**, 93, 39.
- [197] A. J. Opinsky, J. L. Orehtsky, C. W. W. Hoffman, *J. Appl. Phys.* **1962**, 33, 708.
- [198] R. Michel, Y. Bienvenu, A. Chesnaud, A. Thorel, *Int. J. Refract. Met. Hard Mater.* **2020**, 92, 105325.
- [199] G. L. Davis, *Metallurgia* **1958**, 58, 177.
- [200] J. W. Pugh, *Metall. Trans. A* **1980**, 11, 1487.
- [201] F. F. Schmidt, H. R. Ogden, *Defense Metals Information Centre Reports*, Vol. 191, Battelle Memorial Institute, Columbus, OH **1963**, <https://apps.dtic.mil/sti/pdfs/AD0425547.pdf>.
- [202] A. Barna, I. Gaal, O. Geszti-Herkner, G. Radnóczy, L. Uray, *High Temp.- High Pressures* **1978**, 10, 2.
- [203] J. W. Pugh, *Metall. Trans.* **1973**, 4, 553.
- [204] D. L. McDanel, R. A. Signorelli, NASA Technical Note, NASA-TN-D-3467 **1966**.
- [205] B. Harris, E. G. Ellison, *Trans. ASM* **1966**, 59, 744.
- [206] A. Denlevy, J. K. Y. Hum, *SAE Trans.* **1962**, 70, 507.
- [207] J. Conway, P. Flagella, *Physical and Mechanical Properties of Reactor Materials: Seventh Annual Report, AEC Fuels and Materials Development Program* **1968**.
- [208] J. Webb, S. Gollapudi, I. Charit, *Int. J. Refract. Met. Hard Mater.* **2019**, 82, 69.
- [209] W. D. Klopp, W. R. Witzke, *Mechanical Properties and Recrystallization Behavior of Electron-Beam-Melted Tungsten Compared With Arc-Melted Tungsten* **1966**.
- [210] W. Green, *Trans. Metall. Soc. AIME* **1959**, 215, 1058.
- [211] P. Marmy, *Creep-Fatigue of Cu-Cr-Zr: A Review of the Existing Fatigue, Creep and Creep-Fatigue Data Base and a Life Prediction Analysis Using a Time Based Damage Evaluation* **2005**.
- [212] M. F. Ashby, H. J. Frost, *Deformation-Mechanism Maps, The Plasticity and Creep of Metals and Ceramics*, Pergamon Press, UK **1982**.
- [213] M. F. Ashby, H. J. Frost AD-755230 **1972**, <https://apps.dtic.mil/sti/pdfs/AD0755230.pdf> (accessed: July 2024).
- [214] T300 - Standard Modulus Carbon Fiber, <https://www.toraycma.com/wp-content/uploads/T300-Technical-Data-Sheet-1.pdf> (accessed: July 2022).
- [215] E, r and d Glass Properties: Technical Data Sheet, [https://glassproperties.com/glasses/E\\_R\\_and\\_D\\_glass\\_properties.pdf](https://glassproperties.com/glasses/E_R_and_D_glass_properties.pdf) (accessed: July 2022).
- [216] Nicalon, <https://www.coicceramics.com/assets/docs/fiber/nicalon/NICALON.pdf> (accessed: July 2024).
- [217] COI Ceramics Nicalon CG Sico Ceramic Fiber, <https://www.matweb.com/search/datasheet.aspx?matguid=fff771d82eca47129d31a2c81bcaacb1&ckck=1> (accessed: July 2024).



**Johann Riesch** works as a materials scientist at the Max Planck Institute for Plasma Physics (IPP) in Garching on the development and characterization of materials and components for nuclear fusion devices. He has been developing tungsten fibre-reinforced composites ( $W_f/W$ ) for many years and was able to produce the new material for the first time and help establish it in the fusion community and beyond. His focus is now on the fundamental understanding of material behavior in a fusion environment. This includes their mechanical behavior under irradiation and the effects of high heat flux loads.



**Maximilian Fuhr** earned his B.Sc. and M.Sc. in Materials Science and Engineering from Friedrich-Alexander University Erlangen-Nürnberg (FAU) in 2016 and 2019, respectively. He was awarded a Ph.D. in Mechanical Engineering from Technical University of Munich in 2024. The corresponding Ph.D. studies focusing on the deformation mechanisms of drawn tungsten wires were conducted in collaboration with the Max Planck Institute for Plasma Physics in Garching, Germany. He is now working as a senior reliability engineer at Infineon Technologies AG, Neubiberg, Germany.



**Jürgen Almanstötter** is a physicist and principal engineer in the R&D metals department of AMS OSRAM (AMSP LF PRE DMET) at Schwabmünchen, Germany. He received his diploma degree in physics from Technical University of Munich (TUM) and his Ph.D. from University of Stuttgart. Jürgen is with OSRAM for almost 30 years, where he conducted numerous company internal R&D and technology projects. His scientific fields of work covering a broad area ranging from density functional theory (DFT) calculations, microstructural simulations, constitutive material models and multiphysics modeling up to various experimental studies. Some of his research has been published within 20 papers in scientific journals as well as in different contributions at major conferences.